ACADÉMIE
DES SCIENCES
INSTITUT DE FRANCE

Comptes Rendus
Physique

Thomas Chalopin, Igor Ferrier-Barbut, Thierry Lahaye, Antoine Browaeys and David Clément

Connected correlations in cold atom experiments

Volume 27 (2026), p. 65-89

Online since: 25 February 2026

https://doi.org/10.5802/crphys.274

The Comptes Rendus. Physique *are a member of the Mersenne Center for open scientific publishing*
www.centre-mersenne.org — e-ISSN : 1878-1535

ACADÉMIE DES SCIENCES
INSTITUT DE FRANCE

Comptes Rendus. Physique
2026, Vol. 27, p. 65-89
https://doi.org/10.5802/crphys.274

Research article

Connected correlations in cold atom experiments

Thomas Chalopin [*, a], **Igor Ferrier-Barbut** [a], **Thierry Lahaye** [a], **Antoine Browaeys** [a] **and David Clément** [a]

[a] Université Paris-Saclay, Institut d'Optique Graduate School, CNRS, Laboratoire Charles Fabry, 91127 Palaiseau, France

E-mails: thomas.chalopin@institutoptique.fr, igor.ferrier-barbut@institutoptique.fr, thierry.lahaye@institutoptique.fr, antoine.browaeys@institutoptique.fr, david.clement@institutoptique.fr

Abstract. The recent development of single-atom-resolved probes has made full counting statistics measurements accessible in quantum gas experiments. This capability provides access to high-order moments of physical observables, from which cumulants, or equivalently connected correlations, can be precisely determined. Through a selection of recent cold atom experiments, this article illustrates the significance of connected correlations in characterizing ensembles of interacting quantum particles. First, non-zero connected correlations of order $n > 2$ unambiguously identify non-Gaussian quantum states. Second, connected correlations of order n identify clusters made of n elements whose statistical properties are irreducible to combinations of smaller clusters. The ability to identify such multi-particle clusters offers an interesting perspective on strongly correlated quantum states of matter at the microscopic scale.

Keywords. Ultracold atoms, strongly correlated matter, connected correlations, non-Gaussian states.

Funding. This work was supported by the France 2030 program (ANR-22-PETQ-0004, project QuBitAF) the Region Ile-de-France in the framework of the DIM QuanTiP, the European Research Council (Advanced grant No. 101018511-ATARAXIA, ERC StG CORSAIR, 101039361), and the Horizon Europe programme HORIZON-CL4-2022-QUANTUM-02-SGA project 101113690 (PASQuanS2.1).

Note. Article submitted by invitation.

Manuscript received 31 October 2025, revised 20 January 2026, accepted 3 February 2026, online since 25 February 2026.

1. Introduction

Understanding many-body quantum physics remains one of the most formidable challenges in physics [1–5]. While *ab-initio* methods offer a rigorous approach to describing quantum many-body systems from first principles, they are often computationally prohibitive and can obscure the intuitive understanding of the microscopic processes that give rise to macroscopic phenomena. Traditionally, the probing of strongly correlated electronic materials has heavily relied on measuring response functions [6]. Specifically, one-particle spectral functions, obtained through ARPES experiments [7,8], and dynamical structure factors, derived from neutron scattering [9], have been indispensable. These methods effectively probe one-particle (Green functions) and

* Corresponding author

density correlations, offering direct insights into one- and two-body correlations within quantum systems such as superconductors and frustrated magnets, as well as quantum gas experiments [10–15]. However, in strongly correlated matter where higher-order correlations (n-body correlations with $n > 2$) are prevalent, traditional spectral functions serve only as indirect probes, with their shapes and dependence on experimental parameters influenced by higher-order correlations. Extracting the contribution of specific high-order correlations from their spectra often remains a challenge.

Recent advances in detection techniques of synthetic quantum systems of ions [16], atoms [17,18] and superconducting qubits [19,20] have opened new avenues for exploring many-body physics and correlations in experiments through single-particle-resolved probes and measurements of full counting statistics (FCS) [21–28]. Assuming that sufficient statistics is experimentally accessible, these methods offer direct access to higher-order moments of physical observables. Therefore, they provide a means for directly investigating the intricate n-body correlations that define much of strongly correlated condensed matter. By probing individual quantum constituents — such as electrons, atoms, or spins — one may hope to reveal the mechanisms that govern collective quantum behaviour, offering new insights into this complex and fundamental question with respect to other types of measurements.

Measuring high-order moments to identify the contribution of *connected* sets of particles was proposed long ago, beginning with the work of Ursell [29]. In this context, a connected set of n particles designates a group of n particles all correlated with one another, i.e. a group that cannot be described as formed by two (or more) independent sub-groups. In his efforts to better understand classical gases, Ursell aimed at efficiently evaluating Gibbs' phase integral by focusing on specific groupings of molecules — those forming connected clusters. To this aim, he exploited the concept of cumulants of a set of N random variables $\{X_i\}_N$, now referred to as the Ursell function $u(X_1, X_2, \ldots, X_N)$, or the *connected correlation functions* $\langle X_1 X_2 \cdots X_N \rangle_c$. Cumulants isolate genuine correlations: the n-th order cumulant κ_n captures correlations that cannot be explained by lower-order correlations. The key idea of Ursell was to determine a finite (and ideally minimal) number of such cumulants (or connected correlations) that could provide an effective description of the system. The Bogoliubov–Born–Green–Kirkwood–Yvon (BBGKY) hierarchy in classical statistical physics is another example of a similar approach [30]. Identifying a hierarchy in the cumulant contributions was then proven unattainable for strongly correlated bosons at equilibrium [31], but we are not aware of such a conclusion for fermions or spin systems.[1] Hence, an expansion in orders of cumulants does not necessarily provide a viable description of equilibrium many-body states. Nevertheless, cumulants offer a clean, intuitive and physically meaningful way to characterise fluctuations experimentally, especially when dealing with complex or strongly interacting systems.

The present article illustrates two key aspects of cumulants that are useful in the context of strongly correlated quantum matter. A first crucial feature of cumulants or connected correlations is their capability to identify non-Gaussian behaviour: any non-zero cumulant $\kappa_n \neq 0$ of order $n > 2$ indeed reveals the presence of non-Gaussian statistics. In addition to their capability to distinguish Gaussian from non-Gaussian statistics, non-zero cumulants reveal genuine forms of clustering which can help building a physical picture of the system. Their measurements in experiments exploring quantum many-body phases and dynamics has attracted growing interest over the past years. This capability spans a wide range of platforms, including photonic systems, superconducting qubits, trapped ions, and ultracold atoms. This work focuses on recent experiments realised with cold atom systems. It aims to offer a brief, non-exhaustive overview of how connected correlations are measured and employed to uncover both Gaussian and non-Gaussian

[1] Note, however, that a cumulant hierarchy may be found in dynamical many-body systems where the sequential build-up of connected correlations yields reliable predictions over some restricted time windows [32–35].

aspects of quantum states, characterise strongly correlated matter or highlight the relevant features of quasiparticles emerging in interacting systems. Following a short introduction to the concept of cumulants, we highlight their applications in systems of interacting bosons, fermions and spins.

2. Cumulants or connected correlations

2.1. *Definition of cumulants*

Cumulants — connected correlations. The cumulants, or connected correlations, $\kappa_n = \langle X^n \rangle_c$ of a random variable X are defined from their generating function $K_X(t) = \log\left[\langle e^{tX} \rangle\right] = \sum_n \kappa_n t^n / n!$. An example of such a generating function is the free-energy F in statistical physics, defined as $F(\beta) = -1/\beta \log\left(\langle e^{-\beta E} \rangle\right)$ [36], in the canonical ensemble: F is the generating function of the cumulants κ_n of the energy E. The moments $m_n = \langle X^n \rangle$ are related to the cumulants $\kappa_n = \langle X^n \rangle_c$ through the relation

$$m_n = \kappa_n + \sum_{j=1}^{n-1} \frac{(n-1)!}{j!\,(n-1-j)!}\, m_j \kappa_{n-j}. \tag{1}$$

A similar relation relates cumulants to moments.

Of particular interest to the present work is a modified version of the above relation, where the n^{th}-order cumulant κ_n is expressed as a function of the n^{th}-order moment m_n and cumulants of order $n' < n$:

$$\kappa_n = m_n - \sum_{P_j; j=1}^{n-1} \prod_{B \in P_j} \kappa_{|b|} \tag{2}$$

where P_j are all the partitions of n objects into lists B of sub-ensembles whose largest sub-ensemble contains j objects ($|b|$ is the size of the sub-ensembles in the list B). This formula expresses a simple and useful picture of the cumulants [37]: the n^{th}-order cumulant counts the number of connected graphs in a vertex set with n elements. This number is equal to the total number of possible graphs m_n, to which the contributions of connected graphs of order $n' < n$ are subtracted. Therefore, the connected correlations of order n identify the number of connected sets of exactly n correlated elements.

As illustrated in Figure 1, it follows that the connected correlations can be expressed from subtracting from the (total) correlations m_n of order n the contributions from all connected correlations of order $n' < n$. The difference between the total correlations and the connected correlations is referred to as the disconnected correlations (note that disconnected correlations of order n include connected correlations of order $n-1$, $n-2, \ldots$). To complete this illustration, we write the connected correlations of lowest order:

$$\begin{aligned}
\langle X_i \rangle_c &= \langle X_i \rangle, \\
\langle X_i X_j \rangle_c &= \langle X_i X_j \rangle - \langle X_i \rangle_c \langle X_j \rangle_c, \\
\langle X_i X_j X_k \rangle_c &= \langle X_i X_j X_k \rangle - \left(\langle X_i \rangle_c \langle X_j X_k \rangle_c + \langle X_j \rangle_c \langle X_i X_k \rangle_c + \langle X_k \rangle_c \langle X_i X_j \rangle_c \right) - \langle X_i \rangle_c \langle X_j \rangle_c \langle X_j \rangle_c.
\end{aligned}$$

The cumulants of low order have names: mean, variance, skewness and kurtosis for κ_1, κ_2, κ_3 and κ_4 respectively. While the first three cumulants are identical to the centered moments of corresponding order, $\kappa_n = \left\langle \left(X - \langle X \rangle \right)^n \right\rangle$ for $n = 1, 2, 3$, this is not the case anymore from $n > 3$, e.g. $\kappa_4 = \left\langle \left(X - \langle X \rangle \right)^4 \right\rangle - 3\kappa_2^2$.

Cumulants of classical Gaussian random variables. A Gaussian random variable is a random variable whose connected correlations (or cumulants) are zero at any order larger than 2, i.e. $\kappa_n = 0$ for $n > 2$. This definition is equivalent to stating that the knowledge of the mean and standard deviation fully defines a Gaussian random variable. Otherwise stated, connected sets with more than 2 particles are not present in systems with Gaussian statistics.

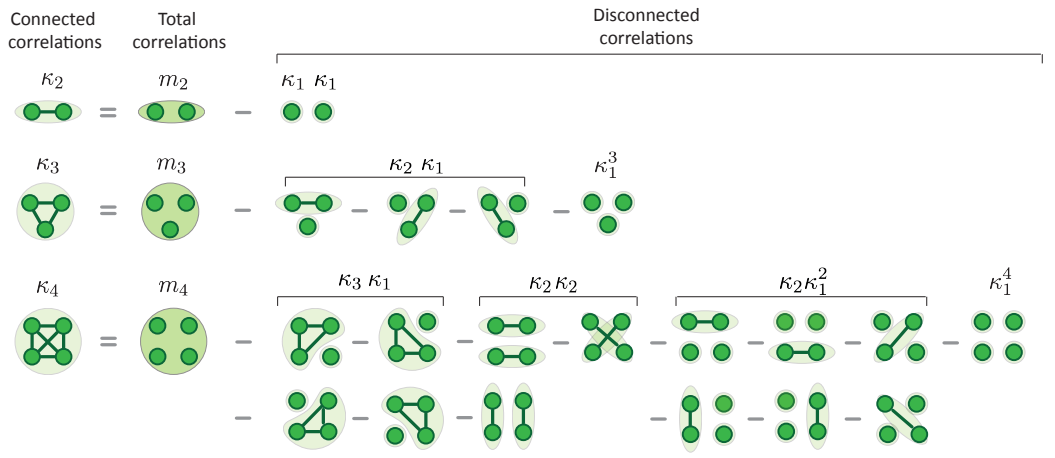

Figure 1. Illustration of the decomposition of cumulants of order n as the difference between the total correlations and all the contributions from cumulants of order $n' < n$ [23].

2.2. *Cumulants of quantum observables*

Connected correlations of quantum states. In the quantum mechanical description, a system is described by a density operator $\widehat{\rho}$ and the statistical average $\langle\cdots\rangle$ of an observable $\widehat{A}$ is $\langle\widehat{A}\rangle = \mathrm{Tr}[\widehat{\rho}\widehat{A}]$. The moments and the cumulants (or connected correlations) of $\widehat{A}$ have the same definition as in the previous paragraph. The cumulant generating function is defined as $K_{\widehat{A}}(\lambda) = \log\left[\langle e^{\lambda\widehat{A}}\rangle\right]$ and cumulants are obtained from its derivatives at $\lambda = 0$. In contrast to the classical case, however, care must be taken in these definitions as the observable $\widehat{A}$ and the Hamiltonian $\widehat{H}$ of the system may not commute, with the consequence that different definitions lead to different results. For instance, at equilibrium where $\widehat{\rho} = e^{-\beta\widehat{H}}/Z$, one may find an alternative, symmetrised definition of the cumulant generating function to the one given here, namely $K_{\widehat{A}}(\lambda) = \log\mathrm{Tr}\left[e^{\lambda\widehat{A}/2}\widehat{\rho}e^{\lambda\widehat{A}/2}\right]$. When $\widehat{A}$ and $\widehat{H}$ do not commute, this alternative definition leads to different values for the cumulants. Similar attention to normal ordering must be paid to the case of an observable $\widehat{A}$ involving non-commuting operators. Its cumulants are obtained from the generating function of the joint cumulants associated to the operators in normal order [38].

Link to normalised correlation functions. In the field of quantum optics, R. Glauber introduced the normalised correlation functions for a light field associated with photon operators [39]. For any creation and annihilation $\widehat{a}^\dagger$ and $\widehat{a}$ (both bosonic and fermionic operators), one can define a normalised correlation function as

$$g^{(n)}(\boldsymbol{x}_1,\ldots,\boldsymbol{x}_n) = \frac{\left\langle \widehat{a}^\dagger(\boldsymbol{x}_1)\cdots\widehat{a}^\dagger(\boldsymbol{x}_n)\widehat{a}(\boldsymbol{x}_n)\cdots\widehat{a}(\boldsymbol{x}_1)\right\rangle}{\left\langle\widehat{I}(\boldsymbol{x}_1)\right\rangle\left\langle\widehat{I}(\boldsymbol{x}_2)\right\rangle\cdots\left\langle\widehat{I}(\boldsymbol{x}_n)\right\rangle} = \frac{G^{(n)}(\boldsymbol{x}_1,\ldots,\boldsymbol{x}_n)}{\left\langle\widehat{I}(\boldsymbol{x}_1)\right\rangle\left\langle\widehat{I}(\boldsymbol{x}_2)\right\rangle\cdots\left\langle\widehat{I}(\boldsymbol{x}_n)\right\rangle}, \tag{3}$$

with $\widehat{I}(\boldsymbol{x}_j) = \widehat{a}^\dagger(\boldsymbol{x}_j)\widehat{a}(\boldsymbol{x}_j)$ the particle number operator at coordinates $\boldsymbol{x}_j = (t_j, \boldsymbol{r}_j)$. Note that the ordering of the creation and annihilation operators plays an important role in the case of fermionic operators. The normalised correlation function $g^{(n)}$ reflects the total correlations and it can be related to the connected correlations using Eq. (2). For instance, the connected "intensity" correlations relates to the normalised two-body correlation function as follows:

$$\left\langle\widehat{I}(\boldsymbol{x}_1)\widehat{I}(\boldsymbol{x}_2)\right\rangle_{\mathrm{c}} = \left[g^{(2)}(\boldsymbol{x}_1,\boldsymbol{x}_2) - 1\right]\left\langle\widehat{I}(\boldsymbol{x}_1)\right\rangle\left\langle\widehat{I}(\boldsymbol{x}_2)\right\rangle + \delta(\boldsymbol{x}_1 - \boldsymbol{x}_2)\left\langle\widehat{I}(\boldsymbol{x}_1)\right\rangle, \tag{4}$$

where $\delta(\boldsymbol{x}_1 - \boldsymbol{x}_2)$ is the Dirac function which is non-zero only when $\boldsymbol{x}_1 = \boldsymbol{x}_2$. In terms of field operators, the normalised two-body correlation function $g^{(2)}$ corresponds to a fourth-order cumulant and contains many contributions (see Figure 1),

$$g^{(2)}(\boldsymbol{x}_1, \boldsymbol{x}_2) \propto \left\langle \hat{a}^\dagger(\boldsymbol{x}_1)\hat{a}^\dagger(\boldsymbol{x}_2)\hat{a}(\boldsymbol{x}_2)\hat{a}(\boldsymbol{x}_1)\right\rangle_{\mathrm{c}} + \left\langle \hat{a}^\dagger(\boldsymbol{x}_1)\hat{a}^\dagger(\boldsymbol{x}_2)\hat{a}(\boldsymbol{x}_2)\right\rangle_{\mathrm{c}}\left\langle \hat{a}(\boldsymbol{x}_1)\right\rangle + \cdots \tag{5}$$

We emphasise that $g^{(2)}$ contains the *total* correlations (see Figure 1), and is an intensive quantity due to its normalisation. For example, in quantum optics, $G^{(2)}$ increases with the intensity, i.e. the number of photons in a temporal mode, while $g^{(2)}$ does not. This contrasts with *connected* correlations $\langle\cdots\rangle_{\mathrm{c}}$ that effectively count the number of connected sets and thus grow with system size. In that regard, connected intensity (or number) correlations can easily be interpreted as the difference between correlated pairs compared to the situation of independent random variables.

2.3. *Motivations for measuring cumulants*

In the present article, we illustrate on a few examples from cold atoms experiments why cumulants are interesting. We have identified two main motivations for measuring cumulants: revealing non-Gaussian quantum states and identifying correlated clusters. In the context of simulating and understanding strongly correlated quantum matter, we believe that these two motivations are extremely fruitful for experiments and represent strong assets associated with the measurements of high-order correlations.

Distinguishing Gaussian from non-Gaussian quantum states. A Gaussian quantum state is a state described by a Gaussian Wigner function, or a Gaussian density matrix [40]. Similarly to the case of a classical Gaussian variable mentioned previously, any connected correlations involving $n \geq 3$ creation/annihilation operators are zero. This implies that a measurement of a non-zero high-order ($n \geq 3$) cumulant of creation/annihilation operators unambiguously indicates that the quantum state is non-Gaussian.

Table 1. Cumulants of operators and their relation to theoretical descriptions of quantum states with increasing number of correlated modes.

Cumulants of operators	Theoretical description	Type of correlations
$\kappa_n = 0$ for $n > 1$	Mean-field theories	No correlations between modes Single-mode correlations induced by quantum statistics
$\kappa_n = 0$ for $n > 2$	Gaussian theories Free quasi-particles theories	Gaussian correlations coupling two modes
$\kappa_n \neq 0$ for $n > 2$	Theories of strongly correlated states	Non-Gaussian correlations between many modes

A parallel can somewhat be drawn with the theoretical description of quantum systems of interacting particles, as illustrated by Table 1. Mean-field theories do not account for quantum fluctuations, establishing equations for one particle in a (classical) field. Therefore they do not include any connected sets of modes.[2] Gaussian theories — such as Bogoliubov theory, Bardeen–Cooper–Schrieffer (BCS) theory and Luttinger liquid theory — include linearised quantum fluctuations that give rise to correlations between two modes. As a result, they can be viewed as approaches considering the contributions of connected sets with up to two modes. Beyond the

[2] A mode is a quantized excitation of a field, associated to a creation/annihilation operator. For instance, a mode in momentum space is associated to the creation operator $\hat{a}_k^\dagger$ of having an excitation with momentum k. The BCS and Bogoliubov theories predict pairing of modes at opposite momenta k/ $-k$ (see below).

linearisation of quantum fluctuations and beyond Gaussian theories, descriptions of strongly correlated quantum matter include the contributions of connected clusters with more than two modes.

From an experimental point of view, correlations between modes (i.e. field correlations) are routinely probed through homodyne and heterodyne interferometers in optics. In contrast, correlations between modes of massive particles are rather revealed indirectly from measuring correlations between particle numbers. This difference between mode correlations and particle correlations has important consequences when identifying the properties of quantum states. For instance, mode entanglement and particle entanglement are not the same [41,42]. Moreover, when attempting to reveal the non-Gaussian nature of a quantum state — defined from a non-zero operator cumulant of order $n > 2$ — measuring two-particle correlations can be sufficient, as it indirectly provides information about 4-mode correlations (see Section 3.2.3).

Identifying correlated clusters. One attempt in understanding correlated quantum matter is to identify the presence of correlated clusters of modes (or particles) at the microscopic level. Celebrated examples are pairing mechanisms at the heart of superconductivity — such as described by Bardeen–Cooper–Schrieffer theory for instance — or superfluidity in liquid Helium-3. Larger correlated clusters involving more than two modes (or particles) are also present in strongly correlated matter, as we shall illustrate below. In experiments, measuring n-body correlations is not sufficient to reveal these microscopic n-uplet clusters — pairs, triplets, quadruplets... — since n-body correlations also include contributions from n'-uplets with $n' < n$ (see Figure 1). Instead, n-order cumulants or connected correlations are the adequate quantities to study as they contain only the genuine contribution from n-uplets. This is illustrated through the fact that (total) n-body correlations $G^{(n)}$ can take non-zero values even in the absence of n-uplet clusters, i.e. when n-body connected correlations $G_{\mathrm{c}}^{(n)}$ are equal to zero.

Continuous phase transitions. The description of phase transitions in statistical physics relies on the scale invariance of the system's fluctuations close to the transition [43]. A well-known consequence of scale invariance is the emergence of algebraic scaling laws for physical quantities, with critical exponents determined by the universality class of the phase transition. This prediction has found experimental confirmation in a large variety of systems ranging from condensed matter to ultracold gases.

Another property deriving from scale invariance is that the statistics of the order parameter assume a universal scaling function. Notably, this universal distribution is expected to be non-Gaussian near the critical point, where fluctuations occur across all spatial scales and the Central Limit Theorem no longer applies [44,45]. Higher-order cumulants of the order parameter are particularly well-suited to uncover the non-Gaussian nature of these fluctuations. However, due to the challenges in measuring high-order cumulants — or equivalently the full probability distribution — of an order parameter, experimental confirmation of its non-Gaussian behaviour at the phase transition remains limited [46].

Recently, the work of Allemand et al. with ultracold lattice bosons exploited high-order cumulants of the condensate order parameter to identify the non-Gaussian critical regime of the superfluid-to-Mott phase transition [47]. In addition, it uncovered universal oscillations of high-order cumulants across phase transitions occurring in finite-size systems. Interestingly, a similar approach could be applied to study various phase transitions, belonging to different universality classes, as several atomic platforms are capable of probing the statistics of order parameters [24–26,48].

3. Models of interacting bosons and fermions

3.1. *Quantum statistics: single-mode correlations*

In the absence of interactions, the unique origin of correlations is quantum statistics. The latter take place within a single mode, resulting in single-mode correlations only. They manifest as a bunching effect in the case of bosons and an anti-bunching effect in the case of fermions. While these correlations are not the ones we are mostly interested to discuss in this article, we briefly comment on them, as well as on the Siegert relation and Wick's theorem [49].

Isserlis' theorem or Wick's theorem relates the moments m_n of a Gaussian variable, or of a Gaussian field, to a combination of moments of order $n' \leq 2$. Such a relation can be derived from the connected correlations: using Eq. (2) and the hypothesis that the statistics is Gaussian, i.e. that any connected correlations of order $n \geq 3$ vanish. Consider for instance two bosonic modes labeled 1 and 2 respectively, with their respective annihilation operators $\hat{a}_1$ and $\hat{a}_2$. The Gaussian nature of the state implies that $\langle \hat{a}_1^\dagger \hat{a}_2^\dagger \hat{a}_2 \hat{a}_1 \rangle_\mathrm{c} = 0$, from which one obtains $\langle \hat{a}_1^\dagger \hat{a}_2^\dagger \hat{a}_2 \hat{a}_1 \rangle = D_4^3 + D_4^2 + D_4^1$ where D_4^j corresponds to the disconnected correlation of order 4 involving connected (operator) correlations of order j (see Figure 1). In the case of an incoherent field, i.e. $\langle \hat{a}_i \rangle = 0$, one has $D_4^3 = D_4^1 = 0$ and $D_4^2 = \left|\langle \hat{a}_1^\dagger \hat{a}_2 \rangle\right|^2 + \langle \hat{a}_1^\dagger \hat{a}_2^\dagger \rangle \langle \hat{a}_1 \hat{a}_2 \rangle + \langle \hat{n}_1 \rangle \langle \hat{n}_2 \rangle$. With the additional assumption $\langle \hat{a}_1 \hat{a}_2 \rangle = 0$ — for instance valid in systems with chaotic statistics or with particle number conservation —, one is left with

$$\langle \hat{a}_1^\dagger \hat{a}_2^\dagger \hat{a}_2 \hat{a}_1 \rangle = \langle \hat{a}_1^\dagger a_1 \rangle \langle a_2^\dagger \hat{a}_2 \rangle + \left|\langle \hat{a}_1^\dagger \hat{a}_2 \rangle\right|^2. \tag{6}$$

This equation is well-known in the context of quantum optics and referred to as the Siegert relation when a single mode is probed. Considering the light emitted by an incoherent source (for which $\langle \hat{a}(t) \rangle = \langle \hat{a}(t)^2 \rangle = 0$ with $\hat{a}(t)$ being a stationary process), it reads

$$g^{(2)}(\delta t) = 1 + \left|g^{(1)}(\delta t)\right|^2 \tag{7}$$

where $g^{(1)}(\delta t) = \langle \hat{a}^\dagger(t) \hat{a}(t+\delta t) \rangle / \sqrt{\langle \hat{a}(t)^\dagger \hat{a}(t) \rangle \langle \hat{a}(t+\delta t)^\dagger \hat{a}(t+\delta t) \rangle}$ characterises the first-order temporal coherence of the source. The above derivation simply relies on the assumption that the light field has Gaussian statistics and zero mean. Chaotic or thermal states, which are often encountered as they result from the incoherent sum of many contributions and application of the Central Limit Theorem [50], share those properties and, in turn, follow the Siegert relation.

When considering a single Gaussian bosonic mode, a similar approach exploiting the structure of connected correlations (equivalent to Wick's theorem) can be applied in the presence of a finite coherence of the field. Using the vanishing of high-order cumulants, e.g. $\langle \hat{a}^\dagger \hat{a}^\dagger \hat{a} \rangle_\mathrm{c} = 0$ and $\langle \hat{a}^\dagger \hat{a}^\dagger \hat{a} \hat{a} \rangle_\mathrm{c} = 0$, a little bit of algebra [51] yields the generic expression

$$\langle \hat{a}^\dagger \hat{a}^\dagger \hat{a} \hat{a} \rangle = \left|\langle \hat{a}^2 \rangle\right|^2 + 2\langle \hat{a}^\dagger \hat{a} \rangle^2 - 2\left|\langle \hat{a} \rangle\right|^4.$$

This expression generalises the Siegert relation (see Eq. (6)) in the case of a single bosonic mode. More specifically, it contains terms with anomalous averages that affect the statistical properties of the state. For a bosonic mode with thermal statistics, one has $\langle \hat{a} \rangle = \langle \hat{a}^2 \rangle = 0$ and one recovers $\langle \hat{a}^\dagger \hat{a}^\dagger \hat{a} \hat{a} \rangle = 2\langle a^\dagger a \rangle^2$, i.e. a perfectly-contrasted bunching. In the case of a coherent state $|\alpha\rangle$ — which is a Gaussian state obtained from the vacuum state $|0\rangle$ by the displacement operator $\hat{D}(\alpha)$, $|\alpha\rangle = D(\alpha)|0\rangle$ — anomalous averages are non-zero. From the properties of the displacement operator, one finds $\langle \hat{a} \rangle = \alpha$ and $\langle \hat{a}^2 \rangle = \alpha^2$, as well as $\langle \hat{a}^\dagger a \rangle = |\alpha|^2$, leading to $\langle \hat{a}^\dagger \hat{a}^\dagger \hat{a} \hat{a} \rangle = |\alpha|^4 = \langle \hat{a}^\dagger \hat{a} \rangle^2$ signaling the absence of bunching. This result is straightforwardly generalised to higher-order correlations in the same mode $\{\boldsymbol{x}_i = \boldsymbol{x}_0\}$, leading to $g^{(n)}\left(\{\boldsymbol{x}_i = \boldsymbol{x}_0\}\right) = 1$ for a coherent state.

For a fermionic mode, one has $\left\langle (\hat{a}^\dagger)^n \hat{a}^n \right\rangle = 0$ for $n \geq 2$ due to Pauli exclusion principle, leading to the fermionic anti-bunching $g^{(n)}\left(\{\boldsymbol{x}_i = \boldsymbol{x}_0\}\right) = 0$ for $n \geq 2$.

The effect of single-mode statistics has been widely probed with ultracold atoms. In direct analogy with the landmark experiments of Hanbury Brown and Twiss [52,53], single-atom-resolved observation of bunching and anti-bunching were reported in atomic gases [27,54–60]. Noise correlation of absorption images was used to unveil underlying spatial ordering, e.g. in lattice systems [61,62]. These implementations of the noise correlation technique suffered from the line-of-sight integration inherent to absorption imaging and from a limited resolution in momentum space. With detection techniques at the single atom level, perfectly-contrasted bunching was observed in thermal Bose gases [58], in the depletion of a condensate [63] and in Mott insulators [64], while perfectly-contrasted anti-bunching was reported in fermionic clouds [58,60,65]. Similar quantitative analysis of the amplitude of correlations induced by quantum statistics were extended to higher-order correlations, enabling a precise characterization of quantum states through their full counting statistics [27,64,66–68].

3.2. *Bosons with contact interactions*

In dilute Bose gases, the atomic density is low enough such that the interaction potential is well approximated by contact interactions, the amplitude of which is set by the two-body s-wave scattering length a_s. The momentum space is a fruitful frame to discuss correlations induced by contact interactions: contact interactions are indeed equivalent to a four-wave mixing term between momentum modes (see illustration in Figure 2(a)). In the following, we consider the Hamiltonian $\widehat{H} = \widehat{H}_0 + \widehat{U}$ with a non-linear (interaction) term $\widehat{U}$ taking the form of a four-wave mixing term, $\widehat{U} \propto \sum_{k_1,k_2,k_3} \widehat{a}^\dagger_{k_1+k_3} \widehat{a}^\dagger_{k_2-k_3} \widehat{a}_{k_1} \widehat{a}_{k_2}$. Note that such a four-wave mixing term is routinely used to describe experiments in ultracold gases [69] as well as in non-linear optics [70].

Recall that the ground-state of an ensemble of ideal bosons is a Bose–Einstein condensate. In the following, the mode of the condensate, i.e. the ground-state of the non-interacting Hamiltonian $\widehat{H}_0$, corresponds to the mode with a momentum equal to zero, $\boldsymbol{k} = \mathbf{0}$.[3]

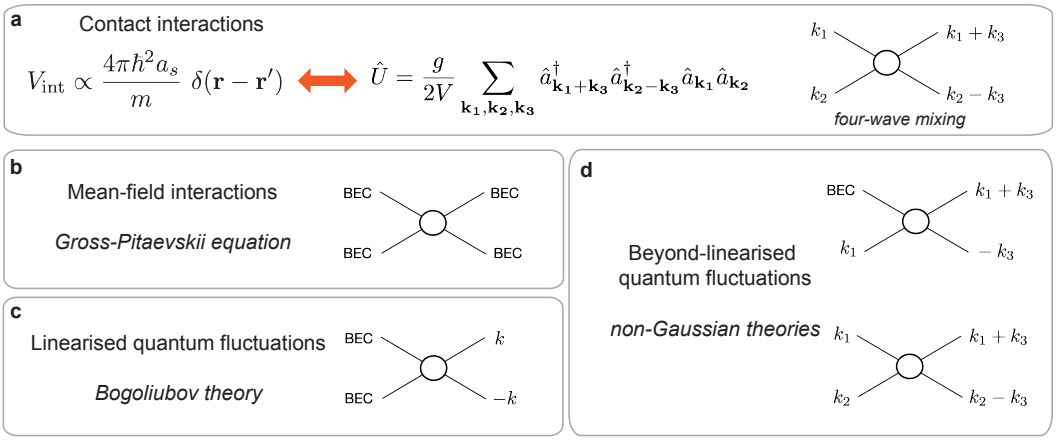

Figure 2. (a) Contact interactions and four-wave mixing in momentum space. Here $g = 4\pi\hbar^2 a_s/m$. (b) Mean-field description of interactions: two-body interactions within the BEC. (c) Linearised quantum fluctuations induced by interactions: creation of momentum-correlated pairs exiting the BEC. (d) Beyond linearised quantum fluctuations: generation of momentum correlation between 3 or 4 different momentum modes.

[3] Identifying the BEC to the mode $\boldsymbol{k} = \mathbf{0}$ is strictly valid only in homogeneous systems with periodic boundary conditions where $\boldsymbol{k}$ is a good quantum number. However, it is an excellent approximation in most experimental configurations.

3.2.1. *Mean-field approximation — Gross–Pitaevskii equation*

The simplest way to account for (contact) interactions is to treat them at the mean-field level. This amounts to neglecting quantum fluctuations between different modes and to considering interactions within the single mode of the BEC (Figure 2(b)). The mean-field ground-state remains the Bose–Einstein condensate (BEC), which however differs from the ground-state of ideal bosons through a modification of its wave-function. The mean-field BEC wave-function is described by a non-linear Schrödinger equation, the Gross–Pitaevskii equation, and the condensate fraction (i.e. the fraction of bosons in the BEC state) is 100% at zero temperature.

In terms of cumulants of (momentum) modes, the mean-field approximation implies that any cumulant of order $n > 1$ is zero. For instance, one has $\langle \widehat{N}^2 \rangle_{\mathrm{c}} = 0$, which implies that $\langle \widehat{N}^2 \rangle = \langle \widehat{N} \rangle^2$. The interaction term, whose sum reduces to the unique contribution of the BEC mode $i = 0$, thus takes the form $\langle \widehat{U} \rangle \propto \langle \widehat{a}_0^\dagger \widehat{a}_0^\dagger \widehat{a}_0 \widehat{a}_0 \rangle = \langle \widehat{N}_0 (\widehat{N}_0 - 1) \rangle = N_0 (N_0 - 1)$ where $N_0 = \langle \widehat{N}_0 \rangle$ is the mean atom number in the BEC mode $\boldsymbol{k} = \boldsymbol{0}$. Note that the amplitude is simply proportional to the number of interacting atom pairs $N_0(N_0 - 1)$.

3.2.2. *Linearised quantum fluctuations — Bogoliubov theory*

Beyond mean-field descriptions include quantum fluctuations that couple different modes at zero temperature (Figure 2(c)–(d)). These quantum fluctuations originate from the non-commutation of the interaction term $\widehat{U}$ with the non-interacting Hamiltonian $\widehat{H}_0$ [71]. They result in the population of modes that are distinct from the BEC, also called the *quantum depletion*. When quantum fluctuations are a small perturbation of the mean-field solution, they are accounted for by linearising their effect in the Hamiltonian (Figure 2(c)). Systems with linearised quantum fluctuations are referred to as weakly interacting ones. In the case of interacting bosons, the theory with linearised quantum fluctuations is the Bogoliubov theory.

Bogoliubov theory assumes the quantum depletion to be small and approximates the operator of the BEC mode to classical field, $\widehat{a}_0 \sim \sqrt{N_0}$ where the average number of bosons in the BEC $N_0 = \langle \widehat{N}_0 \rangle \sim N$ is close to the total number of particles N. The linearisation of quantum fluctuations corresponds to keeping the term $N_0 \sum_{k_1,k_2} \left[\widehat{a}_{k_1}^\dagger \widehat{a}_{k_2}^\dagger + \text{h.c.} \right]$ in the four-wave mixing interactions, in addition to the mean-field contribution. In terms of cumulants, this approach is equivalent to assuming that cumulants of order $n > 2$ are zero. Inserting the condition $\langle \widehat{a}_{k_1}^\dagger \widehat{a}_{k_2}^\dagger \widehat{a}_{k_3} \rangle_{\mathrm{c}} = \langle \widehat{a}_{k_1}^\dagger \widehat{a}_{k_2}^\dagger \widehat{a}_{k_3} \widehat{a}_{k_4} \rangle_{\mathrm{c}} = 0$ in the interaction terms indeed leads to

$$\langle \widehat{U} \rangle \propto N_0 (N_0 - 1) + N_0 \sum_{k_1,k_2} \left[\langle \widehat{a}_{k_1}^\dagger \widehat{a}_{k_2}^\dagger \rangle \langle \widehat{a}_0 \widehat{a}_0 \rangle + \langle \widehat{a}_{k_1}^\dagger \widehat{a}_0^\dagger \rangle \langle \widehat{a}_{k_2} \widehat{a}_0 \rangle + \text{c.c.} \right].$$

The corresponding interacting Hamiltonian is quadratic in operators and can be diagonalised in a basis of quasi-particles. In other words, the system is well described by a Gaussian theory of non-interacting quasi-particles with quantum fluctuations obeying Gaussian statistics. This is identical to stating that the weakly interacting regime is entirely characterised by connected correlations of order $n \leq 2$.

Bogoliubov theory is a celebrated example of such a Gaussian theory that treats quantum fluctuations as linear fluctuations. It predicts that the interaction-induced depletion of the BEC takes the form of two-mode squeezed states at opposite momenta (see Figure 3). Indeed, momentum conservation in the four-wave mixing process implies that $\boldsymbol{k}_2 = -\boldsymbol{k}_1$ in the contribution $N_0 \sum_{\boldsymbol{k}_1,\boldsymbol{k}_2} \left[\widehat{a}_{\boldsymbol{k}_1}^\dagger \widehat{a}_{\boldsymbol{k}_2}^\dagger + \text{h.c.} \right] = N_0 \sum_{\boldsymbol{k}_1} \left[\widehat{a}_{\boldsymbol{k}_1}^\dagger \widehat{a}_{-\boldsymbol{k}_1}^\dagger + \text{h.c.} \right]$.

In the dilute regime $\sqrt{n a_s^3} \ll 1$, Bose gases realise the weakly interacting regime previously described. In addition, these platforms are well suited to probe the momentum-correlated pairs predicted by Bogoliubov theory. Indeed, single-atom-resolved detection methods after a long free expansion from the trap allow one to access the momentum of individual atoms (see [72] for instance), providing access to the full counting statistics of the atom number $N(\boldsymbol{k})$ in the mode $\boldsymbol{k}$.

The presence of two-mode squeezing at opposite momenta can be revealed from measuring *connected* number correlations at opposite momenta,

$$G_{\mathrm{c}}^{(2)}(\boldsymbol{k},-\boldsymbol{k}) = \langle \widehat{N}(\boldsymbol{k})\widehat{N}(-\boldsymbol{k})\rangle - \langle \widehat{N}(\boldsymbol{k})\rangle\langle \widehat{N}(-\boldsymbol{k})\rangle, \tag{8}$$

and finding $G_{\mathrm{c}}^{(2)}(\boldsymbol{k},-\boldsymbol{k}) > 0$. In the experiment of Tenart et al. [57], this signature was used to reveal Bogoliubov pairing in a gas of weakly interacting bosons, as illustrated in Figure 3. The connected correlations are non-zero only in a narrow range of momenta close to the condition $\boldsymbol{k}' = -\boldsymbol{k}$, an experimental evidence of the pairing mechanism between modes at opposite momenta. In such experiments, the momentum is a continuous variable which is measured with a resolution dk smaller than the size Δk of one mode. The size Δk of a mode in momentum space is given by the inverse in-trap size of the gas and it can be measured from the width of the bunching peak in momentum space [63]. This is the case in the data reported in Figure 3: the size of a mode is given by the width of the correlation peak and corresponds here to roughly $\Delta k \sim 10 dk$.

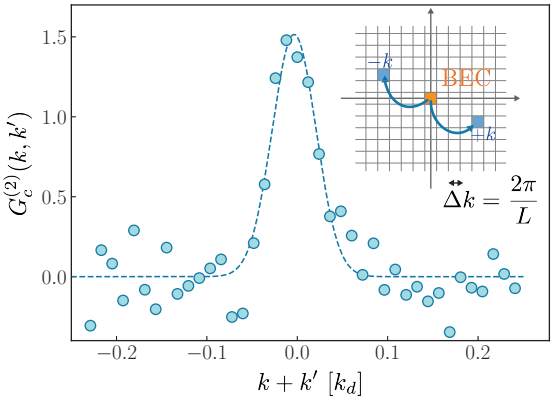

Figure 3. Connected correlations $G_{\mathrm{c}}^{(2)}(\boldsymbol{k},\boldsymbol{k}')$ in the depletion of a weakly interacting condensate as a function of $\boldsymbol{k}+\boldsymbol{k}'$. The data are adapted from [57]. Inset: illustration of two-mode squeezing induced by interactions. A mode in the momentum space occupies a volume Δk^3 where $\Delta k = 2\pi/L$ with L the size of the considered system. The Bose–Einstein condensate (BEC) occupies the mode at $\boldsymbol{k} = \boldsymbol{0}$ and interactions promote Bogoliubov pairs in modes with opposite momenta $\pm\boldsymbol{k}$.

3.2.3. *Non-linearised quantum fluctuations — strongly correlated regime*

When quantum fluctuations become large enough, their effect cannot be linearised and one must resort to non-Gaussian theories. This is the regime of strongly correlated states. The quasi-particles introduced by linearising the effect of quantum fluctuations acquire a finite lifetime in the strongly correlated regime: they are not eigenstates of the interacting Hamiltonian anymore, which implies that they would interact and decay when excited. In other words, a theory of free quasi-particles does not describe the strongly correlated regime.

The non-Gaussian nature of strongly correlated quantum states can in principle be directly revealed from detecting correlated clusters with more than two modes, i.e. from measuring non-zero connected correlations of order $n > 2$ [47]. While measuring high-order correlations in a single bosonic mode has long been achieved [27,66,68], probing correlations between more than two modes remains scarce [64,73]. Alternatively, the measurement of density-density correlations (i.e. two-body correlations) is sometimes sufficient to obtain signatures of non-Gaussianity, as illustrated recently with ultracold interacting Bose gases [74]. In these works, density correlations are used to reveal non-Gaussian statistics in the form of a non-zero fourth-order cumulant of operators.

Non-zero four-operators cumulants. When one considers an ensemble of bosons with no field coherence, $\langle \hat{a}_i \rangle = \langle \hat{a}_i^\dagger \rangle = 0$, the fourth-order cumulant of operators involving two different modes (labeled 1 and 2 respectively) simplifies to

$$\langle \hat{a}_1^\dagger \hat{a}_2^\dagger \hat{a}_2 \hat{a}_1 \rangle_c = \langle \hat{a}_1^\dagger \hat{a}_2^\dagger \hat{a}_2 \hat{a}_1 \rangle - \left| \langle \hat{a}_1^\dagger \hat{a}_2^\dagger \rangle \right|^2 - \left| \langle \hat{a}_1^\dagger \hat{a}_2 \rangle \right|^2 - \langle \hat{N}_1 \rangle \langle \hat{N}_2 \rangle$$

and leads to

$$\langle \hat{N}_1 \hat{N}_2 \rangle_c = \langle \hat{N}_1 \hat{N}_2 \rangle - \langle \hat{N}_1 \rangle \langle \hat{N}_2 \rangle = \langle \hat{a}_1^\dagger \hat{a}_2^\dagger \hat{a}_2 \hat{a}_1 \rangle_c + \left| \langle \hat{a}_1^\dagger \hat{a}_2^\dagger \rangle \right|^2 + \left| \langle \hat{a}_1^\dagger \hat{a}_2 \rangle \right|^2. \tag{9}$$

This relation shows that a measurement of negative connected number correlations, $\langle \hat{N}_1 \hat{N}_2 \rangle_c < 0$, necessarily corresponds to $\langle \hat{a}_1^\dagger \hat{a}_2^\dagger \hat{a}_2 \hat{a}_1 \rangle_c < 0$. Such a non-zero fourth-order cumulant unambiguously indicates that the quantum state is non-Gaussian. In the experiments of Bureik et al. [74], this approach revealed the non-Gaussian nature of momentum correlations in a strongly interacting Bose gas at equilibrium. Note that in the experimental realisation [74], the field coherence was shown to be vanishingly small and compatible with being zero. This example illustrates that information on non-Gaussian correlators that are not an observable may be obtained from the measured connected correlations, upon minimal assumptions.

Absence of a hierarchy in the four-wave mixing processes at strong interactions. As outlined above, there exists a hierarchy in the contributions of the various four-wave mixing processes depicted in Figure 2 within the weakly interacting regime, where the condensate fraction is close to unity ($N_0 \sim N$). Although not strictly zero, the four-wave mixing processes responsible for generating non-Gaussian states are negligible in this regime. In contrast, in the strongly interacting regime, the condensate becomes significantly depleted, and the population of the condensate mode becomes small and comparable to those of the excited modes. As a result, the hierarchical structure of contributions valid in the weakly interacting regime no longer holds and many high-order cumulants have similar contributions.

In the intermediate regime of interactions, where the condensate fraction is appreciably below unity yet remains macroscopic (e.g., ~ 0.5), the hierarchy established for weak interactions may still apply. However, the signatures of non-Gaussianity in the many-body state become appreciable as well, as demonstrated in recent experiments at condensate fractions around ~ 0.75 [74]. This situation shares similarity with the description of the metrological gain in a spin model with a one-axis-twisting term which we discuss in Section 4.1.

3.3. *Interacting fermions*

Interacting fermions lie at the heart of so-called *strongly correlated materials* whose properties heavily depend on interactions between charge carriers. Unconventional superconductors (e.g. cuprate, or "high-T_C" superconductors) constitute a paradigmatic example of such materials. Contrary to conventional superconductors, where phonon-mediated interactions lead to the formation of Cooper pairs [75], the microscopic origin of the pairing instability in unconventional superconductors is not fully understood, but is closely related to strong electron-electron interactions [1].

Ultracold atom platforms provide a particularly convenient way of studying strongly correlated ensembles of fermions over wide ranges of interactions and densities [76]. In early experiments using bulk gases, the formation of Cooper pairs was observed through indirect probes related to superfluid behaviour [77–82]. The rich phenomenology of the BEC-BCS crossover [83], in which the nature of the pairing correlation changes through a Feshbach resonance, has also been extensively explored with global probes, including RF [84] and photoemission spectroscopy [11].

In the scope of this article, we rather focus on a few examples of single-atom resolved experimental explorations of correlations emerging in strongly interacting fermionic systems.

3.3.1. *Correlations in bulk ultracold Fermi gases*

Early measurements of correlations in ultracold Fermi gases dealt with density correlations after expansion of the gas. Superfluidity, for instance, is characterised by a macroscopic population of zero-momentum Cooper pairs. Such pairing is detected by connected correlations between opposite momenta, $\langle \hat{n}(\boldsymbol{k})\hat{n}(-\boldsymbol{k})\rangle_{\mathrm{c}}$ [85], similarly to the Bogoliubov pairing of bosons described above. The formation of local and non-local fermion pairs, in the form of Feshbach molecules, was observed by means of noise correlations in absorption pictures [86]. However, recent experimental efforts led to single-particle detection techniques, allowing to *directly* image such fermionic pairing. This is illustrated in the following two experiments.

Identification of individuals BCS pairs. In the experiment of Holten et al. [87], the ground state of a harmonically trapped Fermi gas with very few particles — a dozen — is studied by measuring the momentum of each constituent (see Figure 4(a)). The presence of pairs of fermions lying close to the Fermi surface (dashed circle) is identified by evaluating the connected correlation function $C^{(2)}(\boldsymbol{p}_\uparrow, \boldsymbol{p}_\downarrow) = \langle \hat{n}_{\boldsymbol{p}_\uparrow}\hat{n}_{\boldsymbol{p}_\downarrow}\rangle_{\mathrm{c}}$, represented in Figure 4(b). There, the cross marks the momentum of the spin-$\downarrow$ particle; a peak in the correlation function is clearly visible at the opposite side of the Fermi surface, as expected from Cooper pairing. In their case, the opposite-momentum correlation peak at the Fermi surface is well reproduced by a mean-field BCS theory.

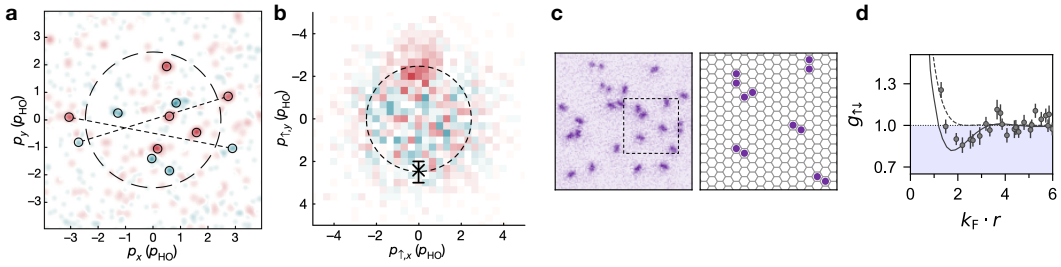

Figure 4. (a) Single-atom spin-resolved measurements of a trapped Fermi gas with $N = 12$ particles in momentum space. The dashed circle indicates the Fermi surface. Momenta are expressed in natural units of the harmonic trap $p_{\mathrm{HO}} = \sqrt{\hbar m\omega}$. (b) Connected correlations $C^{(2)}(\boldsymbol{p}_\uparrow, \boldsymbol{p}_\downarrow)$, where the momentum of the $\downarrow$-fermion is fixed (cross mark). (c) Single-atom resolved measurements of a dilute, strongly interacting Fermi gas in position space. (d) Normalised correlation function $g^{(2)}_{\uparrow\downarrow}(\boldsymbol{r})$ as a function of the distance between opposite-spin fermions, showing a strong peak at short distances and anticorrelations at intermediate distances that is not captured by the mean-field BCS theory (dashed line). The panels (a) and (b) were adapted from [87], while (c) and (d) were adapted from [88].

Spatial correlations. In more recent experiments by Yao et al. [58] and Daix et al. [88], highly dilute two-dimensional Fermi gases are investigated using spatially resolved measurements (Figure 4(c)). As the interaction strength is increased toward the strongly attractive regime, the *normalised* correlation function[4]

$$g^{(2)}_{\uparrow\downarrow}(\boldsymbol{r}) = \frac{\langle \hat{n}_{\boldsymbol{0},\uparrow}\hat{n}_{\boldsymbol{r},\downarrow}\rangle}{\langle \hat{n}_{\boldsymbol{0},\uparrow}\rangle\langle \hat{n}_{\boldsymbol{r},\downarrow}\rangle} \tag{10}$$

develops a pronounced peak as $\boldsymbol{r} \to \boldsymbol{0}$, indicating the emergence of tightly bound local pairs (Figure 4(d)). This behaviour contrasts with the Cooper pairing mechanism, involving states of opposite momenta near the Fermi surface, and is therefore non-local in nature.

[4] Connected and normalised correlation functions are related *via*

$$g^{(2)}_{\uparrow\downarrow}(\boldsymbol{r}) - 1 = \frac{\langle \hat{n}_{\boldsymbol{0},\uparrow}\hat{n}_{\boldsymbol{r},\downarrow}\rangle_{\mathrm{c}}}{\langle \hat{n}_{\boldsymbol{0},\uparrow}\rangle\langle \hat{n}_{\boldsymbol{r},\downarrow}\rangle}.$$

For spin-balanced homogeneous systems $\langle \hat{n}_{\boldsymbol{r},\sigma}\rangle = n$ and $g^{(2)}_{\uparrow\downarrow}(\boldsymbol{r}) - 1 = \langle \hat{n}_{\boldsymbol{0},\uparrow}\hat{n}_{\boldsymbol{r},\downarrow}\rangle_{\mathrm{c}}/n^2$.

Interestingly, in [88] the experimental data additionally shows that *anticorrelations* develop at intermediate distances $k_F r \approx 2$, a feature that is not captured by (mean-field) BCS theory [89] (Figure 4(d)) which neglects interactions in the normal state. The authors attribute this behaviour to non-trivial higher-order correlations. They evaluate in particular the three point correlations

$$g^{(3)}_{\sigma\sigma\sigma'}(r) = \frac{\langle \hat{n}_{\mathbf{0},\sigma}\hat{n}_{\boldsymbol{r}_1,\sigma}\hat{n}_{\boldsymbol{r}_2,\sigma'}\rangle}{\langle \hat{n}_{\mathbf{0},\sigma}\rangle\langle \hat{n}_{\boldsymbol{r}_1,\sigma}\rangle\langle \hat{n}_{\boldsymbol{r}_2,\sigma'}\rangle}, \quad |\boldsymbol{r}_1| = |\boldsymbol{r}_2| = |\boldsymbol{r}_1 - \boldsymbol{r}_2| = r. \tag{11}$$

Their experimental setting only allows measuring such correlations in the case where the three particles are equidistant from each other.

3.3.2. *Ultracold fermions in optical lattices*

Once loaded in optical lattices, assuming the lowest energy band is populated, ultracold atoms naturally realise the Hubbard model [90], originally introduced to describe interacting electrons in solids [91]. In the case of a spin-1/2 system (e.g. when considering two hyperfine states of ^{6}Li or ^{40}K), the Fermi–Hubbard Hamiltonian writes

$$\hat{H} = -t \sum_{\langle \boldsymbol{i},\boldsymbol{j}\rangle,\sigma} \left[\hat{c}^\dagger_{\boldsymbol{i},\sigma}\hat{c}_{\boldsymbol{j},\sigma} + \hat{c}^\dagger_{\boldsymbol{j},\sigma}\hat{c}_{\boldsymbol{i},\sigma}\right] + U\sum_{\boldsymbol{i}} \hat{n}_{\boldsymbol{i},\uparrow}\hat{n}_{\boldsymbol{i},\downarrow}. \tag{12}$$

Here, t and U are the tunneling amplitudes and on-site interaction energies, $\sigma = \uparrow, \downarrow$ is the spin, $\hat{c}_{\boldsymbol{i},\sigma}$ is the annihilation operator for a fermion of spin σ on site $\boldsymbol{i}$, and $\langle \boldsymbol{i}, \boldsymbol{j}\rangle$ designate nearest-neighbour sites.

Antiferromagnetic ordering: two-point correlations. In typical experiments, the Fermi–Hubbard model is studied on a square lattice[5] in the strongly interacting regime where the physics is dominated by the interactions between fermions ($U \gg t$). At half-filling — one fermion per lattice site — and at sufficiently low temperatures, the system develops short-range antiferromagnetic (AFM) ordering in the repulsive case, which is analogous to a charge density wave (CDW), i.e. a staggered checkerboard pattern of empty and doubly occupied sites, in the attractive case.

Antiferromagnetism can be revealed through the measurement of the spin-spin *connected* correlation function

$$C^{(2)}_{\mathrm{ss}}(\boldsymbol{d}) = 4\langle \hat{S}^z_{\mathbf{0}}\hat{S}^z_{\boldsymbol{d}}\rangle_{\mathrm{c}}, \tag{13}$$

where $\hat{S}^z_{\boldsymbol{i}} = (\hat{n}_{\boldsymbol{i},\uparrow} - \hat{n}_{\boldsymbol{i},\downarrow})/2$. This correlator was used in a series of quantum gas microscope experiments [56,93–95], in which locally resolved atomic density measurements allowed to observe magnetic ordering beyond nearest-neighbour. In the Harvard experiment by Mazurenko et al. [95], magnetic correlations extended beyond the system size (Figure 5(a)–(b)).

For $U < 0$, fermions with opposite spins tend to pair-up, leading to the formation of doubly occupied sites (doublons). The symmetries of the attractive model essentially amount to associate empty and doubly occupied sites to the two spin components of the repulsive model; AFM ordering thus translates to a CDW in the form of a checkerboard pattern, identified through a density correlations $C^{(2)}_{\mathrm{nn}}(\boldsymbol{d}) = \langle \hat{n}_{\mathbf{0}}\hat{n}_{\boldsymbol{d}}\rangle_{\mathrm{c}}$. First observations of such correlations were reported in [96]. There, correlations are evaluated as a function of local density at $U/t \approx -5$. More recently, the MIT experiment by Hartke et al. [97] (Figure 5(c)–(d)) which studied the same physics with increasing interaction strength, observed that these correlations peak around $U/t \approx -8$.

In the context of the Fermi–Hubbard model, two point correlations have also been explored in alternative geometries. In triangular lattices [98,99], the emergence of magnetic ordering is strongly affected by frustration. Evidence of pairing between dopants has also been reported in so-called mixed-dimensional geometries [100,101].

[5] On a bipartite-lattice (such as a square lattice), the Fermi–Hubbard model is particle-hole symmetric. Consequently, the phase diagram of the attractive and repulsive cases ($U < 0$ and $U > 0$ respectively) are similar in nature [92].

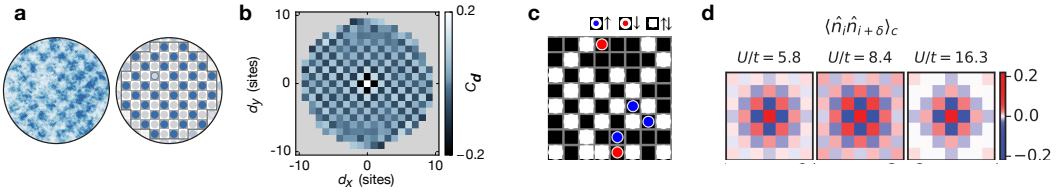

Figure 5. (a) Quantum gas microscopy of a repulsive Fermi–Hubbard system close to half-filling, with one spin component removed. (b) Resulting spin correlation map, computed using Eq. (13), displaying significant correlations across the entire system. Panels (a) and (b) were extracted and adapted from [95]. (c) Quantum gas microscopy of an attractive Fermi–Hubbard system. (d) Resulting density correlations, exhibiting a checkerboard pattern characteristic of CDW ordering, analogous to the AFM ordering of the repulsive case. Note that this *connected* correlator takes negative values precisely because the disconnected part is subtracted. Panels (c) and (d) were extracted and adapted from [97].

Highligthing the physics of dopants: three-point spin-charge correlations. A variety of strongly correlated phases emerge upon doping, i.e. when adding or removing fermions [102]. Over the past few years, considerable experimental interest has been devoted to the physics of weakly doped antiferromagnets, in a regime associated with the emergence of so-called *magnetic polarons*. In the framework of condensed-matter physics, polarons are quasiparticles with well-defined excitation spectra, which have been predicted to emerge around mobile dopants in the Fermi–Hubbard model [103]. From the point of view of quantum gas microscope experiments, where the position of the spins and the dopants can be measured, these polarons are often described as single dopants "dressed" by the background antiferromagnet [104].

Third-order spin-charge *connected* correlation functions (Figure 6(a)) are well suited to characterise the spatial features of these objects, and have been used in numerous recent experiments on the square [97,105–107] and triangular [108,109] lattice. Here, the quantity of interest is

$$C^{(3)}_{\mathrm{dss}}(\boldsymbol{r},\boldsymbol{d}) = \frac{4\langle \widehat{d}_{\mathbf{0}} \widehat{S}^z_{\boldsymbol{r}_1} \widehat{S}^z_{\boldsymbol{r}_2} \rangle_{\mathrm{c}}}{\langle \widehat{d}_{\mathbf{0}} \rangle}, \quad \text{with} \quad \begin{cases} (\boldsymbol{r}_1 + \boldsymbol{r}_2)/2 = \boldsymbol{r} \\ \boldsymbol{r}_2 - \boldsymbol{r}_1 = \boldsymbol{d}. \end{cases} \tag{14}$$

This correlation function quantifies how much the (second-order) spin correlations $\widehat{S}^z_{\boldsymbol{r}_1} \widehat{S}^z_{\boldsymbol{r}_2}$ are affected by the presence of a dopant $\widehat{d}_{\mathbf{0}}$ nearby.[6] Remarkably, these *connected* correlations reveal genuine three-body objects composed of a single dopant and two spins, whose existence only relies on two-body interactions.

First usage of these correlation functions was reported in the experiment by Koepsell et al. [106], where the *bare* correlator was used. Their study was focused on answering the question: what are the spin correlations *conditioned* on the presence of a nearby dopant — in their case a doubly occupied site. Their analysis thus consisted in calculating the connected two-point correlation $C^{(2)}_{\mathrm{ss}}(\boldsymbol{d})$ on post-selected data where the dopant is separated by a distance $\boldsymbol{r}$ to the spin-bond. This procedure is equivalent to computing the normalised correlator of Eq. (14), without removing the disconnected part. Note that, in a spin-balanced system ($\langle \widehat{S}^z_{\boldsymbol{i}} \rangle = 0$), one finds $C^{(3)}_{\mathrm{dss}}(\boldsymbol{r},\boldsymbol{d}) = 4\langle \widehat{d}_{\mathbf{0}} \widehat{S}^z_{\boldsymbol{r}_1} \widehat{S}^z_{\boldsymbol{r}_2} \rangle / \langle \widehat{d}_{\mathbf{0}} \rangle - 4\langle \widehat{S}^z_{\boldsymbol{r}_1} \widehat{S}^z_{\boldsymbol{r}_2} \rangle$. In other words, one recovers that the disconnected part of the correlator corresponds to the spin correlation being agnostic to the presence of the dopant. An example of a connected correlation map is illustrated in Figure 6(a), for NN ($|\boldsymbol{d}| = 1$) and NNN ($|\boldsymbol{d}| = \sqrt{2}$) spin bonds.

More recent studies focused on three-point correlations on the triangular lattice, which break particle-hole symmetry. There, doublon- and hole-doped systems are completely different. In

[6] Here, the dopant takes a different definition depending on whether the system is hole-doped ($\widehat{d}_{\boldsymbol{i}} = (1-\hat{n}_{\boldsymbol{i},\uparrow})(1-\hat{n}_{\boldsymbol{i},\uparrow})$) or doublon-doped ($\widehat{d}_{\boldsymbol{i}} = \hat{n}_{\boldsymbol{i},\uparrow}\hat{n}_{\boldsymbol{i},\downarrow}$).

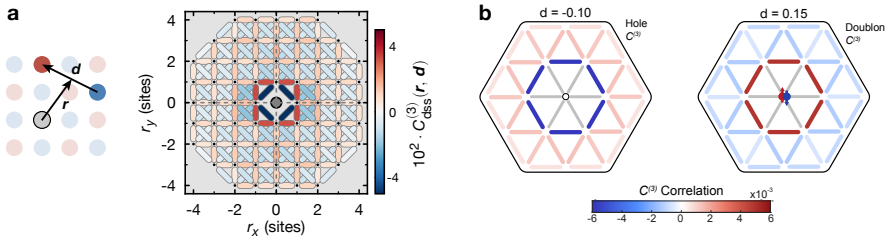

Figure 6. (a) Third order dopant-spin-spin correlations measured with a square-lattice Fermi–Hubbard microscope. In this example (extracted from [105]), significant connected correlations are observed to relatively large distances $|\boldsymbol{r}|$ from the dopant. Only NN ($|\boldsymbol{d}| = 1$) and NNN ($|\boldsymbol{d}| = \sqrt{2}$) spin-bonds are represented. (b) Third order correlations on a triangular lattice (panel adapted from [109]). Here, the breaking of particle-hole symmetry leads to a strong asymmetry between hole- and doublon-doped systems.

the former case, the presence of doublons favors alignment of neighbouring spins and is associated to so-called Nagaoka ferromagnetism, while in the latter case, the presence of holes enhances antiferromagnetism [109,110] (Figure 6(b)). On a triangular lattice, magnetic properties are dominated by the kinetic energy — or motion — of the particles, as opposed to the superexchange energy on a bipartite lattice, and enhance considerably the emergence of magnetic polarons [111].

Higher-order correlations: strongly correlated regime. While second order spin or charge correlations are routinely measured in solid state physics through response functions, third-order correlations that characterise the spatial structure of magnetic polarons are inaccessible in condensed matter devices. For this reason, higher-order (connected) correlations, which by nature characterise strongly correlated states, have until recently remained elusive to theoretical and experimental condensed matter research. The power of quantum gas microscopes, and more generally of experiments with single particle detection capabilities, is precisely the ability to measure *connected* correlation functions, in principle up to arbitrary order. Nevertheless, the measurement and interpretation of correlation functions beyond second or third order in the Fermi–Hubbard model remains mostly exploratory. The regime where such higher-order correlation functions become significant, in particular, was only reached in recent work — either by change of the lattice structure [109], or through systematic explorations of doped systems at relatively low temperature [105,107]. On the theoretical side, studies that start exploring higher-order correlation functions and their use to characterise strongly correlated states remain very scarce [112,113].

4. Spin models

Spin models also constitute an important class of many-body systems receiving a large attention in the context of quantum simulation and computing, but also for quantum metrology. The general idea of quantum metrology is to harness quantum many-body effects — e.g. correlations and entanglement — as a resource for enhancing the sensitivity of measurements. Intuitively, the regime where entanglement becomes macroscopic corresponds to the strongly correlated regime, in which higher-order cumulants become significant. In this section, we discuss two different spin systems, the One-Axis-Twisting (OAT) Hamiltonian relevant in particular for the generation of spin squeezing, and the case of dissipative spins, in which non-trivial correlations due to collective dissipation emerge. In both cases, the presence of non-Gaussian states can be revealed through a cumulant analysis (see e.g. [114,115]).

4.1. *One-Axis-Twisting (OAT) Hamiltonian*

The one-axis-twisting Hamiltonian $\widehat{H} = \chi \widehat{J}_x^2$ is an example of a non-linear Hamiltonian useful for metrology [116–118]. It has been implemented in different atomic systems, most often aiming at generating spin-squeezed states with enhanced metrological precision [21,119–127]. Actually, interactions in the OAT model do not generate only spin squeezing in Gaussian states, but they also lead to stronger correlations and non-Gaussian states in certain regimes [128]. Here we use this OAT model to illustrate that cumulants are well suited to capture various regimes of correlations generated by interactions. Furthermore, this study also gives the opportunity to discuss the presence, or absence, of a hierarchy in the cumulants. We will base our discussion on the experimental results of [128], obtained using Dy atoms in the ground manifold which have spin $J = 8$.

The dynamics of a large spin under the OAT Hamiltonian generates a Gaussian, squeezed state at early times [116]. Such a squeezed state reduces the uncertainty (or "squeezes" the noise) in one variable below the standard quantum limit (at the expense of increasing the uncertainty in its conjugate variable). Squeezed states have the potential to lead to a metrological gain $\overline{G} = 1/\xi^2$ characterised by the so-called squeezing parameter ξ [117,129]. The squeezing parameter is defined as $\xi^2 = 2J\Delta J_{\mathrm{min}}^2/\langle \widehat{J} \rangle^2$, where ΔJ_{min} represents the variance of the spin projected along the axis where it is minimal (i.e. the "squeezed" variable). Beyond the early dynamics, the OAT creates non-Gaussian states, for instance a cat state $\left(|J,+J\rangle + |J,-J\rangle\right)/\sqrt{2}$ at a time $t = \pi/2\chi$ [130]. In the case of non-Gaussian states, the sensitivity to an external field can be enhanced, even with a large spin variance. Generally, the metrological gain is not defined by the squeezing parameter, but rather by the Hellinger distance that measures the similarity between two probability distributions [122,128].

The difference between the regimes where one can assume a Gaussian state and use the squeezing parameter to evaluate the metrological gain, and the one where this assumption breaks down is highlighted in Figure 7(a) adapted from [128]. Both the metrological gain given by the squeezing parameter ($\overline{G}$) and the generalised one (G) are plotted as a function of duration t of the OAT dynamics. While their values coincide at early times, $t/\tau \leq 0.5$, the squeezing parameter is unable to capture the metrological gain associated with the regime of non-Gaussian states.

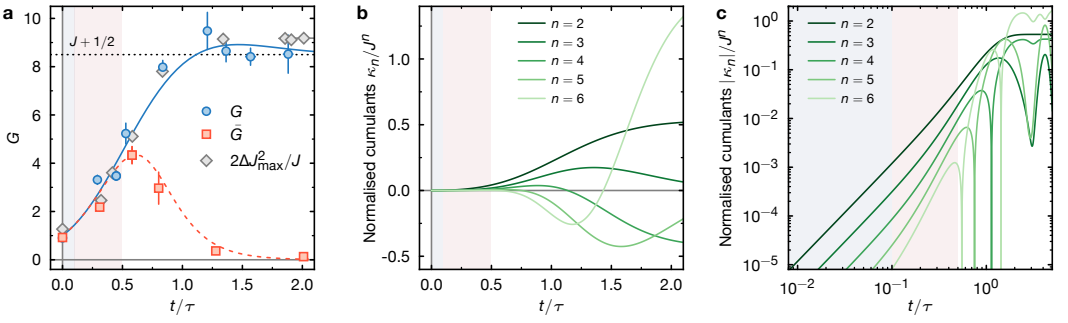

Figure 7. (a) Dynamics of the squeezing (Gaussian) metrological gain $\overline{G}$ and of the generalised (non-Gaussian) gain G, defined from the Hellinger distance. $\tau = (\sqrt{2}J\chi)^{-1}$ is the time scale of the OAT dynamics. The solid and dashed lines are theoretical predictions. The markers are measurements reported in [128]. (b) Normalised cumulants of the operator $\widehat{J}_z$ as a function of time. The n^{th}-order cumulant $\kappa_n \equiv \langle \widehat{J}_z^n \rangle_{\mathrm{c}}$ is normalised by the n^{th} power of the total spin length, J^n. (c) Same plot as in (b) in log-log scale. In all the panels, the blue shaded area corresponds to early times $0 \leq t/\tau \leq 0.1$ for which the hierarchy of cumulants is well-established and stationary. The red shaded area corresponds to intermediate times $0.1 \leq t/\tau \leq 0.5$ where the hierarchy, although still valid, evolves significantly. At later times $t/\tau \geq 0.5$, no hierarchy can be identified.

We now discuss the OAT dynamics through the time evolution of the cumulants of the operator $\widehat{J}_z$, rather than the metrological gain. Those are plotted in Figure 7(b)–(c). For very small evolution durations, $t/\tau \leq 0.1$ (blue regions in Figure 7), a well-defined hierarchy in the cumulants is found, with $\kappa_{n+1} \ll \kappa_n$ for $n \geq 2$ (see Figure 7(c)). In this regime, neglecting the contributions from cumulants of order larger than $n = 2$ is an excellent approximation. This is the regime where the Gaussian approximation holds, accounting only for linearised fluctuations and considering Gaussian states (see Section 3.2.2). As expected, the metrological gain is given by squeezing $G \simeq \overline{G}$ in this regime. Although negligible at these short dynamics, high-order cumulants always take finite values. At intermediate durations, $0.1 \leq t/\tau \leq 0.5$ (red region in Figure 7), the hierarchy in the cumulants is conserved. However, the amplitudes of high-order cumulants $n > 2$ approach that of the second-order cumulant, with the consequence that neglecting the contributions from high-order cumulants is not a good approximation anymore. This implies that quantum states are not well approximated with Gaussian states and that the metrological gain G starts departing from that given by the squeezing parameter $\overline{G}$ (see Figure 7(a)). At later times, $0.5 \leq t/\tau$, the hierarchy of the cumulants breaks down, with high-order ones $n \geq 3$ contributing similarly to the $n = 2$ cumulant. The gains G and $\overline{G}$ strongly differ as well. This regime corresponds to a strongly correlated regime where non-Gaussian correlations play a central role in the physical properties. Importantly, we find that, similarly to the expectations for bosons [31], no hierarchy in the cumulants exists in the strongly correlated regime for the considered system of interacting spins.

4.2. *Dissipative spin models*

As a last example, we consider a spin system with collective dissipation. There, one is interested in the emergence of correlations as a result of the collective dissipation. One situation where this could occur is Dicke superradiance [131], where one considers an ensemble of identical two-level atoms with permutational symmetry. In this case, starting from a fully inverted system, Dicke showed that correlations of the type $\langle \widehat{\sigma}_i^+ \widehat{\sigma}_j^- \rangle$ emerge due to collective spontaneous emission while the individual dipole of each atom remains zero, i.e. $\langle \widehat{\sigma}_i^- \rangle = 0$ [132]. More generally, the question of how correlations form in a dissipative spin system when collective dissipation competes with an external driving field is the topic of intense investigation [34,133–139].

We will focus here on one type of dissipative spin system: two-level atoms coupled to each other via their dipole radiation and collectively dissipating by spontaneous emission. The usual treatment of this problem traces out the field degrees of freedom and results in a master equation for the two-level atoms' density matrix [140]. Solving the full master equation to describe the dynamics is out of reach. As a consequence, one resorts to approximations to describe the system's dynamics and/or steady state. One such approximation is to perform a cumulant expansion, truncated at a given order [34,141–144]. In particular, it is known that the superradiant pulse, even in large ensembles outside of the Dicke regime can be well described by mean-field dynamics, with fluctuations playing a role mostly at the beginning of the pulse [132], which can be captured by a second-order (Gaussian) truncation. Increasing the truncation order is rapidly very costly numerically, and it remains a challenge to perform beyond Gaussian simulations despite recent progress, for instance considering systems with spatial symmetries [145]. In addition, it is known that a cumulant expansion might fail [115], for instance to describe some observables in specific regimes such as the density matrix of the system during subradiance due to the presence of high-order correlations [137]. Another theoretical method, which does not truncate the cumulant expansion but somehow assumes that correlations do not grow strongly during the dynamics is the truncated Wigner approximation, which has been adapted for spin models recently [146,147], and has been successful at describing the dynamics of atoms

radiating collectively via a nano-fiber waveguide [148,149]. From the experimental point of view, measuring cumulants is useful if one wants to flag the appearance of correlations in the ensembles. As we will see below it is also a natural byproduct of measurements of the statistics of the radiated light.

To relate collective light scattering to correlations in atomic ensembles, we write the expression of the electric field emitted by the ensemble in terms of atomic operators:

$$\widehat{E}^{+}(\boldsymbol{R}) = \sum_{n} G(\boldsymbol{R}-\boldsymbol{r}_n)\widehat{\sigma}_n^{-}, \tag{15}$$

where $G(\boldsymbol{R}-\boldsymbol{r}_n)$ is the Green's function for propagation of the electric field [150]. From this one obtains the intensity $I = \langle \widehat{E}^{-}\widehat{E}^{+}\rangle$ emitted by N atoms in a direction $\boldsymbol{e}_k$:

$$I_N(\boldsymbol{e}_k) = I_1(\boldsymbol{e}_k)\sum_{m,n} e^{-i\boldsymbol{k}\cdot(\boldsymbol{r}_n-\boldsymbol{r}_m)}\langle \widehat{\sigma}_n^{+}\widehat{\sigma}_m^{-}\rangle. \tag{16}$$

Here, $\boldsymbol{k} = k_0\boldsymbol{e}_k$, $k_0 = 2\pi/\lambda_0$ is the wavevector corresponding to the atomic transition and $I_1(\boldsymbol{e}_k)$ is the intensity emitted by a single isolated atom. Equation (16) shows that the presence of two-atom correlations with the right phase factor can enhance the intensity emanating from an atomic ensemble in a particular direction. This is how Dicke superradiance results in a stronger emission than that of independent atoms. The observation of a superradiant burst of light [151–155] from an initially inverted cloud of atoms (i.e. in a product state where all atoms are in the excited state $|e\rangle$) indicates the spontaneous appearance of two-atom correlations. Since during the decay $\langle \widehat{\sigma}_n^{+}\rangle = 0$, it directly reveals a non-zero second-order cumulant $\langle \widehat{\sigma}_n^{+}\widehat{\sigma}_m^{-}\rangle \neq \langle \widehat{\sigma}_n^{+}\rangle\langle \widehat{\sigma}_m^{-}\rangle$.

At this level, the state of the light field radiated by the ensemble may still be described as a Gaussian field. However, preparing quantum non-Gaussian field states is an outstanding goal of quantum optics [156–159], motivating the investigation of correlations beyond second order. The natural experimental observable to look at is thus the second-order correlation function $g^{(2)}(\delta t)$ [160,161]. Its measurement during a superradiant pulse was performed recently, both in free-space atomic ensembles [162] and with atoms coupled to a nanofiber [149]: there, the transition from $g^{(2)}(0) \simeq 2$ to $g^{(2)}(0) \simeq 1$ revealed that superradiance establishes correlations between the emitting dipoles. Finally, we note that to be a useful source of non-Gaussian light for quantum optics, one also has to demonstrate its "quantumness", i.e. Wigner negativity.

5. Conclusion

This article covered a few recent examples of ultracold atoms experiments measuring connected correlations in quantum many-body systems of bosons, fermions and of spins. Through these examples, it illustrates how microscopic connected correlations are well suited to characterizing quantum many-body states in the strongly correlated regime. More precisely, they unveil non-Gaussian features — those that go beyond the predictions of free quasi-particle theories — and they reveal the presence of correlated clusters involving more than two particles or modes. The ability to measure such high-order connected correlations is a direct consequence of the single-particle detection capabilities of modern experiments using synthetic quantum systems. As such, the ideas presented in this article apply to other platforms as well, including trapped ions [21,163], Rydberg atoms [164], superconducting qubits [165] and photonic systems [156,166].

Beyond the identification of non-Gaussianity and correlated clusters discussed here, strongly correlated states are also often expected to exhibit entanglement. However, characterizing macroscopic entanglement properties in quantum many-body systems remains a significant challenge. In connection to this article, we find it interesting to ask whether the measurement of connected correlations could also prove useful in this context. For instance, in the case of Gaussian states, such as squeezed states, connected correlations have proven to be valuable

tools [167,168]. Nevertheless, multipartite-entangled states typically exhibit non-Gaussian features [119,122], and the extent to which connected correlations can meaningfully capture entanglement in the strongly correlated regime remains an open and active question. Moreover, the connection between generalized fluctuations of particles (i.e. high-order cumulants or FCS) and entanglement entropy has been explored in several theoretical studies [169–171], but remains to be approached experimentally.

Acknowledgments

We acknowledge stimulating and insightful discussions with Maxime Allemand, Alain Aspect, Denis Boiron, Servaas Kokkelmans, Martin Zwierlein and the *Quantum Gases* group at Institut d'Optique. We thank Tarik Yefsah for providing Figure 4(c) and (d).

Declaration of interests

The authors do not work for, advise, own shares in, or receive funds from any organization that could benefit from this article, and have declared no affiliations other than their research organizations.

References

[1] E. Morosan, D. Natelson, A. H. Nevidomskyy and Q. Si, "Strongly Correlated Materials", *Adv. Mater.* **24** (2012), no. 36, pp. 4896–4923.
[2] I. M. Georgescu, S. Ashhab and F. Nori, "Quantum simulation", *Rev. Mod. Phys.* **86** (2014), no. 1, pp. 153–185.
[3] T. Langen, R. Geiger and J. Schmiedmayer, "Ultracold Atoms Out of Equilibrium", *Ann. Rev. Cond. Matter Phys.* **6** (2015), pp. 201–217.
[4] C. Monroe, W. C. Campbell, L.-M. Duan, et al., "Programmable quantum simulations of spin systems with trapped ions", *Rev. Mod. Phys.* **93** (2021), no. 2, article no. 025001 (57 pages).
[5] T. Grass, D. Bercioux, U. Bhattacharya, M. Lewenstein, H. S. Nguyen and C. Weitenberg, "Colloquium: Synthetic quantum matter in nonstandard geometries", *Rev. Mod. Phys.* **97** (2025), no. 1, article no. 011001 (31 pages).
[6] D. N. Basov, R. D. Averitt, D. van der Marel, M. Dressel and K. Haule, "Electrodynamics of correlated electron materials", *Rev. Mod. Phys.* **83** (2011), no. 2, pp. 471–541.
[7] A. Damascelli, Z. Hussain and Z.-X. Shen, "Angle-resolved photoemission studies of the cuprate superconductors", *Rev. Mod. Phys.* **75** (2003), no. 2, pp. 473–541.
[8] J. A. Sobota, Y. He and Z.-X. Shen, "Angle-resolved photoemission studies of quantum materials", *Rev. Mod. Phys.* **93** (2021), no. 2, article no. 025006 (72 pages).
[9] S. Mühlbauer, D. Honecker, É. A. Périgo, et al., "Magnetic small-angle neutron scattering", *Rev. Mod. Phys.* **91** (2019), no. 1, article no. 015004 (75 pages).
[10] T.-L. Dao, A. Georges, J. Dalibard, C. Salomon and I. Carusotto, "Measuring the One-Particle Excitations of Ultracold Fermionic Atoms by Stimulated Raman Spectroscopy", *Phys. Rev. Lett.* **98** (2007), no. 24, article no. 240402 (4 pages).
[11] J. T. Stewart, J. P. Gaebler and D. S. Jin, "Using photoemission spectroscopy to probe a strongly interacting Fermi gas", *Nature* **454** (2008), no. 7205, pp. 744–747.
[12] G. Veeravalli, E. Kuhnle, P. Dyke and C. J. Vale, "Bragg Spectroscopy of a Strongly Interacting Fermi Gas", *Phys. Rev. Lett.* **101** (2008), no. 25, article no. 250403 (4 pages).
[13] D. Clément, N. Fabbri, L. Fallani, C. Fort and M. Inguscio, "Bragg Spectroscopy of Strongly Correlated Bosons in Optical Lattices", *J. Low Temp. Phys.* **158** (2009), no. 1, pp. 5–15.
[14] R. A. Hart, P. M. Duarte, T.-L. Yang, et al., "Observation of Antiferromagnetic Correlations in the Hubbard Model with Ultracold Atoms", *Nature* **519** (2015), no. 7542, pp. 211–214.
[15] H.-J. Shao, Y.-X. Wang, D.-Z. Zhu, et al., "Antiferromagnetic phase transition in a 3D fermionic Hubbard model", *Nature* **632** (2024), no. 8024, pp. 267–272.
[16] C. Monroe and J. Kim, "Scaling the Ion Trap Quantum Processor", *Science* **339** (2013), no. 6124, pp. 1164–1169.
[17] H. Ott, "Single atom detection in ultracold quantum gases: a review of current progress", *Rep. Prog. Phys.* **79** (2016), no. 5, article no. 054401.

[18] C. Gross and W. S. Bakr, "Quantum gas microscopy for single atom and spin detection", *Nat. Phys.* **17** (2021), no. 12, pp. 1316–1323.

[19] M. H. Devoret and R. J. Schoelkopf, "Superconducting Circuits for Quantum Information: An Outlook", *Science* **339** (2013), no. 6124, pp. 1169–1174.

[20] M. Kjaergaard, M. E. Schwartz, J. Braumüller, P. Krantz, J. I.-J. Wang, S. Gustavsson and W. D. Oliver, "Superconducting Qubits: Current State of Play", *Ann. Rev. Cond. Matter Phys.* **11** (2020), pp. 369–395.

[21] J. G. Bohnet, B. C. Sawyer, J. W. Britton, M. L. Wall, A. M. Rey, M. Foss-Feig and J. J. Bollinger, "Quantum spin dynamics and entanglement generation with hundreds of trapped ions", *Science* **352** (2016), no. 6291, pp. 1297–1301.

[22] T. Schweigler, V. Kasper, S. Erne, et al., "Experimental characterization of a quantum many-body system via higher-order correlations", *Nature* **545** (2017), no. 7654, pp. 323–326.

[23] M. Rispoli, A. Lukin, R. Schittko, S. Kim, M. E. Tai, J. Léonard and M. Greiner, "Quantum critical behaviour at the many-body localization transition", *Nature* **573** (2019), no. 7774, pp. 385–389.

[24] V. Makhalov, T. Satoor, A. Evrard, T. Chalopin, R. Lopes and S. Nascimbene, "Probing Quantum Criticality and Symmetry Breaking at the Microscopic Level", *Phys. Rev. Lett.* **123** (2019), no. 12, article no. 120601 (6 pages).

[25] S. Ebadi, T. T. Wang, H. Levine, et al., "Quantum phases of matter on a 256-atom programmable quantum simulator", *Nature* **595** (2021), no. 7866, pp. 227–232.

[26] C. Chen, G. Bornet, M. Bintz, et al., "Continuous symmetry breaking in a two-dimensional Rydberg array", *Nature* **616** (2023), no. 7958, pp. 691–695.

[27] G. Hercé, J.-P. Bureik, A. Ténart, A. Aspect, A. Dareau and D. Clément, "Full counting statistics of interacting lattice gases after an expansion: The role of condensate depletion in many-body coherence", *Phys. Rev. Res.* **5** (2023), no. 1, article no. L012037 (6 pages).

[28] L. K. Joshi, F. Ares, M. K. Joshi, C. F. Roos and P. Calabrese, "Measuring Full Counting Statistics in a Trapped-Ion Quantum Simulator", *Phys. Rev. Lett.* **135** (2025), article no. 160601 (6 pages).

[29] H. D. Ursell, "The evaluation of Gibbs' phase-integral for imperfect gases", *Math. Proc. Camb. Philos. Soc.* **23** (1927), no. 6, pp. 685–697.

[30] L. E. Reichl, *A modern course in statistical physics*, 4th edition, John Wiley & Sons, 1998.

[31] D. W. Robinson, "A theorem concerning the positive metric", *Commun. Math. Phys.* **1** (1965), no. 1, pp. 89–94.

[32] S. Krönke and P. Schmelcher, "Born–Bogoliubov–Green–Kirkwood–Yvon hierarchy for ultracold bosonic systems", *Phys. Rev. A* **98** (2018), article no. 013629 (36 pages).

[33] S. Musolino, H. Kurkjian, M. Van Regemortel, M. Wouters, S. J. J. M. F. Kokkelmans and V. E. Colussi, "Bose–Einstein Condensation of Efimovian Triples in the Unitary Bose Gas", *Phys. Rev. Lett.* **128** (2022), article no. 020401 (8 pages).

[34] W. Verstraelen, D. Huybrechts, T. Roscilde and M. Wouters, "Quantum and Classical Correlations in Open Quantum Spin Lattices via Truncated-Cumulant Trajectories", *PRX Quantum* **4** (2023), no. 3, article no. 030304 (28 pages).

[35] J. van de Kraats, D. J. M. Ahmed-Braun, V. E. Colussi and S. J. J. M. F. Kokkelmans, "Nonequilibrium dynamics and atom-pair coherence in strongly interacting Bose–Fermi mixtures", *Phys. Rev. Res.* **6** (2024), article no. 043016 (14 pages).

[36] K. Huang, *Statistical Mechanics*, John Wiley & Sons, 1987.

[37] J. Novak, "Three lectures on free probability", in *Random matrix theory, interacting particle systems, and integrable systems* (P. Deift and P. Forrester, eds.), Mathematical Sciences Research Institute Publications, vol. 65, Cambridge University Press, 2014, pp. 309–383.

[38] H. J. Carmichael, *Statistical Methods in Quantum Optics 2: Non-classical Fields*, Theoretical and Mathematical Physics, Springer, 2008.

[39] R. J. Glauber, "The Quantum Theory of Optical Coherence", *Phys. Rev.* **130** (1963), no. 6, pp. 2529–2539.

[40] C. W. Gardiner and P. Zoller, *Quantum noise: a handbook of Markovian and non-Markovian quantum stochastic methods with applications to quantum optics*, Springer Series in Synergetics, Springer, 2004.

[41] R. Horodecki, P. Horodecki, M. Horodecki and K. Horodecki, "Quantum entanglement", *Rev. Mod. Phys.* **81** (2009), no. 2, pp. 865–942.

[42] B. Morris, B. Yadin, M. Fadel, T. Zibold, P. Treutlein and G. Adesso, "Entanglement between Identical Particles Is a Useful and Consistent Resource", *Phys. Rev. X* **10** (2020), no. 4, article no. 041012 (26 pages).

[43] H. Nishimori and G. Ortiz, *Elements of Phase Transitions and Critical Phenomena*, Oxford Graduate Texts, Oxford University Press, 2010.

[44] J.-P. Bouchaud and A. Georges, "Anomalous diffusion in disordered media: Statistical mechanisms, models and physical applications", *Phys. Rep.* **195** (1990), no. 4, pp. 127–293.

[45] I. Balog, A. Rançon and B. Delamotte, "Critical Probability Distributions of the Order Parameter from the Functional Renormalization Group", *Phys. Rev. Lett.* **129** (2022), article no. 210602 (6 pages).

[46] S. Joubaud, A. Petrosyan, S. Ciliberto and N. B. Garnier, "Experimental Evidence of Non-Gaussian Fluctuations near a Critical Point", *Phys. Rev. Lett.* **100** (2008), no. 18, article no. 180601 (4 pages).

[47] M. Allemand, G. Dupuy, P. Paquiez, N. Dupuis, A. Rançon, T. Roscilde, T. Chalopin and D. Clément, "Observation of Universal Non-Gaussian Statistics of the Order Parameter across a Continuous Phase Transition", preprint, 2025. Online at https://arxiv.org/abs/2508.21623.

[48] J. Ho, Y.-H. Lu, T. Xiang, C. C. Rusconi, S. J. Masson, A. Asenjo-Garcia, Z. Yan and D. M. Stamper-Kurn, "Optomechanical self-organization in a mesoscopic atom array", *Nat. Phys.* **21** (2025), pp. 1–7.

[49] C. Cohen-Tannoudji and C. Robilliard, "Wave Functions, Relative Phase and Interference for Atomic Bose–Einstein Condensates", *Comptes Rendus. Physique* **2** (2001), no. 3, pp. 445–477.

[50] J. W. Goodman, *Statistical optics*, Wiley Series in Pure and Applied Optics, John Wiley & Sons, 2015.

[51] R. Kubo, "Generalized Cumulant Expansion Method", *J. Phys. Soc. Japan* **17** (1962), no. 7, pp. 1100–1120.

[52] R. Hanbury Brown and R. Q. Twiss, "Correlation between Photons in two Coherent Beams of Light", *Nature* **177** (1956), no. 4497, pp. 27–29.

[53] R. Hanbury Brown and R. Q. Twiss, "A Test of a New Type of Stellar Interferometer on Sirius", *Nature* **178** (1956), no. 4541, pp. 1046–1048.

[54] M. Schellekens, R. Hoppeler, A. Perrin, J. V. Gomes, D. Boiron, A. Aspect and C. I. Westbrook, "Hanbury-Brown–Twiss Effect for Ultracold Quantum Gases", *Science* **310** (2005), no. 5748, pp. 648–651.

[55] T. Jeltes, J. M. McNamara, W. Hogervorst, et al., "Comparison of the Hanbury-Brown–Twiss effect for bosons and fermions", *Nature* **445** (2007), no. 7126, pp. 402–405.

[56] L. W. Cheuk, M. A. Nichols, K. R. Lawrence, et al., "Observation of spatial charge and spin correlations in the 2D Fermi–Hubbard model", *Science* **353** (2016), no. 6305, pp. 1260–1264.

[57] A. Tenart, G. Hercé, J.-P. Bureik, A. Dareau and D. Clément, "Observation of pairs of atoms at opposite momenta in an equilibrium interacting Bose gas", *Nat. Phys.* **17** (2021), no. 12, pp. 1364–1368.

[58] R. Yao, S. Chi, M. Wang, R. J. Fletcher and M. W. Zwierlein, "Measuring Pair Correlations in Bose and Fermi Gases via Atom-Resolved Microscopy", *Phys. Rev. Lett.* **134** (2025), no. 18, article no. 183402 (7 pages).

[59] J. Xiang, E. Cruz-Colón, C. C. Chua, W. R. Milner, J. de Hond, J. F. Fricke and W. Ketterle, "In Situ Imaging of the Thermal de Broglie Wavelength in an Ultracold Bose Gas", *Phys. Rev. Lett.* **134** (2025), no. 18, article no. 183401 (6 pages).

[60] T. de Jongh, J. Verstraten, M. Dixmerias, C. Daix, B. Peaudecerf and T. Yefsah, "Quantum Gas Microscopy of Fermions in the Continuum", *Phys. Rev. Lett.* **134** (2025), no. 18, article no. 183403 (7 pages).

[61] S. Fölling, F. Gerbier, A. Widera, O. Mandel, T. Gericke and I. Bloch, "Spatial quantum noise interferometry in expanding ultracold atom clouds", *Nature* **434** (2005), no. 7032, pp. 481–484.

[62] T. Rom, T. Best, D. van Oosten, U. Schneider, S. Fölling, B. Paredes and I. Bloch, "Free fermion antibunching in a degenerate atomic Fermi gas released from an optical lattice", *Nature* **444** (2006), no. 7120, pp. 733–736.

[63] H. Cayla, S. Butera, C. Carcy, et al., "Hanbury Brown and Twiss Bunching of Phonons and of the Quantum Depletion in an Interacting Bose Gas", *Phys. Rev. Lett.* **125** (2020), no. 16, article no. 165301 (6 pages).

[64] C. Carcy, H. Cayla, A. Tenart, A. Aspect, M. Mancini and D. Clément, "Momentum-Space Atom Correlations in a Mott Insulator", *Phys. Rev. X* **9** (2019), no. 4, article no. 041028 (13 pages).

[65] P. M. Preiss, J. H. Becher, R. Klemt, V. M. Klinkhamer, A. Bergschneider, N. Defenu and S. Jochim, "High-Contrast Interference of Ultracold Fermions", *Phys. Rev. Lett.* **122** (2019), no. 14, article no. 143602 (6 pages).

[66] R. G. Dall, A. G. Manning, S. S. Hodgman, W. RuGway, K. V. Kheruntsyan and A. G. Truscott, "Ideal n-body correlations with massive particles", *Nat. Phys.* **9** (2013), no. 6, pp. 341–344.

[67] M. Holten, L. Bayha, K. Subramanian, C. Heintze, P. M. Preiss and S. Jochim, "Observation of Pauli Crystals", *Phys. Rev. Lett.* **126** (2021), no. 2, article no. 020401 (5 pages).

[68] K. F. Thomas, S. Li, A. H. Abbas, A. G. Truscott and S. S. Hodgman, "N-body antibunching in a degenerate Fermi gas of ^{3}He* atoms", *Phys. Rev. Res.* **6** (2024), no. 2, article no. L022003 (9 pages).

[69] L. Pitaevskii and S. Stringari, *Bose–Einstein condensation and superfluidity*, International Series of Monographs on Physics, vol. 164, Oxford University Press, 2016.

[70] P. D. Drummond and M. Hillery, *The quantum theory of nonlinear optics*, Cambridge University Press, 2014.

[71] L. Pitaevskii and S. Stringari, "Uncertainty principle, quantum fluctuations, and broken symmetries", *J. Low Temp. Phys.* **85** (1991), no. 5, pp. 377–388.

[72] H. Cayla, C. Carcy, Q. Bouton, R. Chang, G. Carleo, M. Mancini and D. Clément, "Single-atom-resolved probing of lattice gases in momentum space", *Phys. Rev. A* **97** (2018), no. 6, article no. 061609 (5 pages).

[73] S. S. Hodgman, R. I. Khakimov, R. J. Lewis-Swan, A. G. Truscott and K. V. Kheruntsyan, "Solving the Quantum Many-Body Problem via Correlations Measured with a Momentum Microscope", *Phys. Rev. Lett.* **118** (2017), no. 24, article no. 240402 (6 pages).

[74] J.-P. Bureik, G. Hercé, M. Allemand, A. Tenart, T. Roscilde and D. Clément, "Suppression of Bogoliubov momentum pairing and emergence of non-Gaussian correlations in ultracold interacting Bose gases", *Nat. Phys.* **21** (2025), no. 1, pp. 57–62.

[75] J. Bardeen, L. N. Cooper and J. R. Schrieffer, "Microscopic Theory of Superconductivity", *Phys. Rev.* **106** (1957), no. 1, pp. 162–164.
[76] W. Ketterle and M. W. Zwierlein, "Making, probing and understanding ultracold Fermi gases", *Riv. Nuovo Cim.* **31** (2008), no. 506, pp. 247–422.
[77] T. Bourdel, L. Khaykovich, J. Cubizolles, et al., "Experimental Study of the BEC-BCS Crossover Region in Lithium 6", *Phys. Rev. Lett.* **93** (2004), no. 5, article no. 050401 (4 pages).
[78] M. Greiner, C. A. Regal and D. S. Jin, "Emergence of a molecular Bose–Einstein condensate from a Fermi gas", *Nature* **426** (2003), no. 6966, pp. 537–540.
[79] S. Jochim, M. Bartenstein, A. Altmeyer, G. Hendl, S. Riedl, C. Chin, J. Hecker Denschlag and R. Grimm, "Bose–Einstein Condensation of Molecules", *Science* **302** (2003), no. 5653, pp. 2101–2103.
[80] M. W. Zwierlein, C. A. Stan, C. H. Schunck, S. M. F. Raupach, S. Gupta, Z. Hadzibabic and W. Ketterle, "Observation of Bose–Einstein Condensation of Molecules", *Phys. Rev. Lett.* **91** (2003), no. 25, article no. 250401 (4 pages).
[81] M. W. Zwierlein, J. R. Abo-Shaeer, A. Schirotzek, C. H. Schunck and W. Ketterle, "Vortices and superfluidity in a strongly interacting Fermi gas", *Nature* **435** (2005), no. 7045, pp. 1047–1051.
[82] M. W. Zwierlein, A. Schirotzek, C. H. Schunck and W. Ketterle, "Fermionic Superfluidity with Imbalanced Spin Populations", *Science* **311** (2006), no. 5760, pp. 492–496.
[83] M. Randeria, W. Zwerger and M. W. Zwierlein, "The BCS-BEC Crossover and the Unitary Fermi Gas", in *The BCS-BEC Crossover and the Unitary Fermi Gas* (W. Zwerger, ed.), Lecture Notes in Physics, vol. 836, Springer, 2012, pp. 1–32.
[84] C. Chin, M. Bartenstein, A. Altmeyer, S. Riedl, S. Jochim, J. H. Denschlag and R. Grimm, "Observation of the Pairing Gap in a Strongly Interacting Fermi Gas", *Science* **305** (2004), no. 5687, pp. 1128–1130.
[85] E. Altman, E. Demler and M. D. Lukin, "Probing many-body states of ultracold atoms via noise correlations", *Phys. Rev. A* **70** (2004), no. 1, article no. 013603 (4 pages).
[86] M. Greiner, C. A. Regal, J. T. Stewart and D. S. Jin, "Probing Pair-Correlated Fermionic Atoms through Correlations in Atom Shot Noise", *Phys. Rev. Lett.* **94** (2005), no. 11, article no. 110401 (4 pages).
[87] M. Holten, L. Bayha, K. Subramanian, S. Brandstetter, C. Heintze, P. Lunt, P. M. Preiss and S. Jochim, "Observation of Cooper pairs in a mesoscopic two-dimensional Fermi gas", *Nature* **606** (2022), no. 7913, pp. 287–291.
[88] C. Daix, M. Dixmerias, Y.-Y. He, J. Verstraten, T. d. Jongh, B. Peaudecerf, S. Zhang and T. Yefsah, "Observing Spatial Charge and Spin Correlations in a Strongly-Interacting Fermi Gas", preprint, 2025. Online at https://arxiv.org/abs/2504.01885.
[89] J. C. Obeso-Jureidini and V. Romero-Rochín, "Density correlation functions and the spatial structure of the two-dimensional BEC-BCS crossover", *Phys. Rev. A* **105** (2022), no. 4, article no. 043307 (14 pages).
[90] D. Jaksch, C. Bruder, J. I. Cirac, C. W. Gardiner and P. Zoller, "Cold Bosonic Atoms in Optical Lattices", *Phys. Rev. Lett.* **81** (1998), no. 15, pp. 3108–3111.
[91] J. Hubbard and B. H. Flowers, "Electron correlations in narrow energy bands", *Proc. R. Soc. Lond., A, Math. Phys. Eng. Sci.* **276** (1963), no. 1365, pp. 238–257.
[92] A. F. Ho, M. A. Cazalilla and T. Giamarchi, "Quantum simulation of the Hubbard model: The attractive route", *Phys. Rev. A* **79** (2009), no. 3, article no. 033620 (11 pages).
[93] M. F. Parsons, A. Mazurenko, C. S. Chiu, G. Ji, D. Greif and M. Greiner, "Site-resolved measurement of the spin-correlation function in the Fermi–Hubbard model", *Science* **353** (2016), no. 6305, pp. 1253–1256.
[94] M. Boll, T. A. Hilker, G. Salomon, A. Omran, J. Nespolo, L. Pollet, I. Bloch and C. Gross, "Spin- and density-resolved microscopy of antiferromagnetic correlations in Fermi–Hubbard chains", *Science* **353** (2016), no. 6305, pp. 1257–1260.
[95] A. Mazurenko, C. S. Chiu, G. Ji, et al., "A cold-atom Fermi–Hubbard antiferromagnet", *Nature* **545** (2017), no. 7655, pp. 462–466.
[96] D. Mitra, P. T. Brown, E. Guardado-Sanchez, S. S. Kondov, T. Devakul, D. A. Huse, P. Schauss and W. S. Bakr, "Quantum gas microscopy of an attractive Fermi–Hubbard system", *Nat. Phys.* **14** (2018), no. 2, pp. 173–177.
[97] T. Hartke, B. Oreg, C. Turnbaugh, N. Jia and M. W. Zwierlein, "Direct observation of nonlocal fermion pairing in an attractive Fermi–Hubbard gas", *Science* **381** (2023), no. 6653, pp. 82–86.
[98] M. Xu, L. H. Kendrick, A. Kale, Y. Gang, G. Ji, R. T. Scalettar, M. Lebrat and M. Greiner, "Frustration- and doping-induced magnetism in a Fermi–Hubbard simulator", *Nature* **620** (2023), no. 7976, pp. 971–976.
[99] J. Mongkolkiattichai, L. Liu, D. Garwood, J. Yang and P. Schauss, "Quantum gas microscopy of fermionic triangular-lattice Mott insulators", *Phys. Rev. A* **108** (2023), no. 6, article no. L061301 (6 pages).
[100] D. Bourgund, T. Chalopin, P. Bojović, et al., "Formation of individual stripes in a mixed-dimensional cold-atom Fermi–Hubbard system", *Nature* **637** (2025), no. 8044, pp. 57–62.
[101] S. Hirthe, T. Chalopin, D. Bourgund, et al., "Magnetically mediated hole pairing in fermionic ladders of ultracold atoms", *Nature* **613** (2023), no. 7944, pp. 463–467.
[102] M. Qin, T. Schäfer, S. Andergassen, P. Corboz and E. Gull, "The Hubbard Model: A Computational Perspective", *Ann. Rev. Cond. Matter Phys.* **13** (2022), no. 1, pp. 275–302.

[103] C. L. Kane, P. A. Lee and N. Read, "Motion of a single hole in a quantum antiferromagnet", *Phys. Rev. B* **39** (1989), no. 10, pp. 6880–6897.

[104] F. Grusdt, M. Kánasz-Nagy, A. Bohrdt, C. S. Chiu, G. Ji, M. Greiner, D. Greif and E. Demler, "Parton Theory of Magnetic Polarons: Mesonic Resonances and Signatures in Dynamics", *Phys. Rev. X* **8** (2018), no. 1, article no. 011046 (39 pages).

[105] T. Chalopin, P. Bojović, S. Wang, et al., "Observation of emergent scaling of spin–charge correlations at the onset of the pseudogap", *Proc. Natl. Acad. Sci. USA* **123** (2026), no. 4, article no. e2525539123 (8 pages).

[106] J. Koepsell, J. Vijayan, P. Sompet, et al., "Imaging magnetic polarons in the doped Fermi–Hubbard model", *Nature* **572** (2019), no. 7769, pp. 358–362.

[107] J. Koepsell, D. Bourgund, P. Sompet, et al., "Microscopic evolution of doped Mott insulators from polaronic metal to Fermi liquid", *Science* **374** (2021), no. 6563, pp. 82–86.

[108] M. Lebrat, M. Xu, L. H. Kendrick, et al., "Observation of Nagaoka polarons in a Fermi–Hubbard quantum simulator", *Nature* **629** (2024), no. 8011, pp. 317–322.

[109] M. L. Prichard, B. M. Spar, I. Morera, E. Demler, Z. Z. Yan and W. S. Bakr, "Directly imaging spin polarons in a kinetically frustrated Hubbard system", *Nature* **629** (2024), no. 8011, pp. 323–328.

[110] M. Lebrat, A. Kale, L. H. Kendrick, M. Xu, Y. Gang, A. Nikolaenko, S. Sachdev and M. Greiner, "Ferrimagnetism of ultracold fermions in a multi-band Hubbard system", preprint, 2024. Online at https://arxiv.org/abs/2404.17555.

[111] I. Morera, A. Bohrdt, W. W. Ho and E. Demler, "Attraction from kinetic frustration in ladder systems", *Phys. Rev. Res.* **6** (2024), no. 2, article no. 023196 (18 pages).

[112] A. Bohrdt, Y. Wang, J. Koepsell, M. Kánasz-Nagy, E. Demler and F. Grusdt, "Dominant Fifth-Order Correlations in Doped Quantum Antiferromagnets", *Phys. Rev. Lett.* **126** (2021), no. 2, article no. 026401 (7 pages).

[113] T. Müller, R. Thomale, S. Sachdev and Y. Iqbal, "Polaronic correlations from optimized ancilla wave functions for the Fermi–Hubbard model", *Proc. Natl. Acad. Sci. USA* **122** (2025), no. 20, article no. e2504261122 (7 pages).

[114] F. Carollo, "Non-Gaussian Dynamics of Quantum Fluctuations and Mean-Field Limit in Open Quantum Central Spin Systems", *Phys. Rev. Lett.* **131** (2023), no. 22, article no. 227102 (8 pages).

[115] P. Fowler-Wright, K. B. Arnardóttir, P. Kirton, B. W. Lovett and J. Keeling, "Determining the validity of cumulant expansions for central spin models", *Phys. Rev. Res.* **5** (2023), no. 3, article no. 033148 (9 pages).

[116] M. Kitagawa and M. Ueda, "Squeezed spin states", *Phys. Rev. A* **47** (1993), no. 6, pp. 5138–5143.

[117] D. J. Wineland, J. J. Bollinger, W. M. Itano and D. J. Heinzen, "Squeezed atomic states and projection noise in spectroscopy", *Phys. Rev. A* **50** (1994), no. 1, pp. 67–88.

[118] J. Ma, X. Wang, C. P. Sun and F. Nori, "Quantum spin squeezing", *Phys. Rep.* **509** (2011), no. 2, pp. 89–165.

[119] L. Pezzè, A. Smerzi, M. K. Oberthaler, R. Schmied and P. Treutlein, "Quantum metrology with nonclassical states of atomic ensembles", *Rev. Mod. Phys.* **90** (2018), no. 3, article no. 035005 (70 pages).

[120] M. F. Riedel, P. Böhi, Y. Li, T. W. Hänsch, A. Sinatra and P. Treutlein, "Atom-Chip-Based Generation of Entanglement for Quantum Metrology", *Nature* **464** (2010), no. 7292, pp. 1170–1173.

[121] C. Gross, T. Zibold, E. Nicklas, J. Estève and M. K. Oberthaler, "Nonlinear atom interferometer surpasses classical precision limit", *Nature* **464** (2010), no. 7292, pp. 1165–1169.

[122] H. Strobel, W. Muessel, D. Linnemann, T. Zibold, D. B. Hume, L. Pezzè, A. Smerzi and M. K. Oberthaler, "Fisher information and entanglement of non-Gaussian spin states", *Science* **345** (2014), no. 6195, pp. 424–427.

[123] I. D. Leroux, M. H. Schleier-Smith and V. Vuletić, "Implementation of Cavity Squeezing of a Collective Atomic Spin", *Phys. Rev. Lett.* **104** (2010), no. 7, article no. 073602 (4 pages).

[124] M. A. Norcia, R. J. Lewis-Swan, J. R. K. Cline, B. Zhu, A. M. Rey and J. K. Thompson, "Cavity-mediated collective spin-exchange interactions in a strontium superradiant laser", *Science* **361** (2018), no. 6399, pp. 259–262.

[125] B. Braverman, A. Kawasaki, E. Pedrozo-Peñafiel, et al., "Near-Unitary Spin Squeezing in ^{171}Yb", *Phys. Rev. Lett.* **122** (2019), no. 22, article no. 223203 (6 pages).

[126] E. Pedrozo-Peñafiel, S. Colombo, C. Shu, et al., "Entanglement on an optical atomic-clock transition", *Nature* **588** (2020), no. 7838, pp. 414–418.

[127] J. Franke, S. R. Muleady, R. Kaubruegger, F. Kranzl, R. Blatt, A. M. Rey, M. K. Joshi and C. F. Roos, "Quantum-Enhanced Sensing on Optical Transitions through Finite-Range Interactions", *Nature* **621** (2023), no. 7980, pp. 740–745.

[128] A. Evrard, V. Makhalov, T. Chalopin, L. A. Sidorenkov, J. Dalibard, R. Lopes and S. Nascimbene, "Enhanced Magnetic Sensitivity with Non-Gaussian Quantum Fluctuations", *Phys. Rev. Lett.* **122** (2019), no. 17, article no. 173601 (6 pages).

[129] D. J. Wineland, J. J. Bollinger, W. M. Itano, F. L. Moore and D. J. Heinzen, "Spin squeezing and reduced quantum noise in spectroscopy", *Phys. Rev. A* **46** (1992), no. 11, R6797–R6800.

[130] T. Chalopin, C. Bouazza, A. Evrard, V. Makhalov, D. Dreon, J. Dalibard, L. A. Sidorenkov and S. Nascimbene, "Quantum-enhanced sensing using non-classical spin states of a highly magnetic atom", *Nat. Commun.* **9** (2018), no. 1, article no. 4955 (8 pages).

[131] R. H. Dicke, "Coherence in Spontaneous Radiation Processes", *Phys. Rev.* **93** (1954), no. 1, pp. 99–110.
[132] M. Gross and S. Haroche, "Superradiance: An essay on the theory of collective spontaneous emission", *Phys. Rep.* **93** (1982), no. 5, pp. 301–396.
[133] T. E. Lee, S. Gopalakrishnan and M. D. Lukin, "Unconventional Magnetism via Optical Pumping of Interacting Spin Systems", *Phys. Rev. Lett.* **110** (2013), no. 25, article no. 257204 (5 pages).
[134] B. Olmos, D. Yu and I. Lesanovsky, "Steady-state properties of a driven atomic ensemble with nonlocal dissipation", *Phys. Rev. A* **89** (2014), no. 2, article no. 023616 (6 pages).
[135] C. D. Parmee and N. R. Cooper, "Phases of driven two-level systems with nonlocal dissipation", *Phys. Rev. A* **97** (2018), no. 5, article no. 053616 (9 pages).
[136] C. D. Parmee and J. Ruostekoski, "Signatures of Optical Phase Transitions in Superradiant and Subradiant Atomic Arrays", *Commun. Phys.* **3** (2020), no. 1, article no. 205 (11 pages).
[137] L. Henriet, J. S. Douglas, D. E. Chang and A. Albrecht, "Critical Open-System Dynamics in a One-Dimensional Optical-Lattice Clock", *Phys. Rev. A* **99** (2019), no. 2, article no. 023802 (20 pages).
[138] K. C. Stitely, F. Finger, R. Rosa-Medina, F. Ferri, T. Donner, T. Esslinger, S. Parkins and B. Krauskopf, "Quantum Fluctuation Dynamics of Dispersive Superradiant Pulses in a Hybrid Light-Matter System", *Phys. Rev. Lett.* **131** (2023), no. 14, article no. 143604 (7 pages).
[139] O. Rubies-Bigorda, S. J. Masson, S. F. Yelin and A. Asenjo-Garcia, "Deterministic Generation of Photonic Entangled States Using Decoherence-Free Subspaces", *Phys. Rev. Lett.* **134** (2025), no. 21, article no. 213603 (7 pages).
[140] R. H. Lehmberg, "Radiation from an N-Atom System. I. General Formalism", *Phys. Rev. A* **2** (1970), no. 3, pp. 883–888.
[141] P. Kirton, M. M. Roses, J. Keeling and E. G. Dalla Torre, "Introduction to the Dicke Model: From Equilibrium to Nonequilibrium, and Vice Versa", *Adv. Quantum Technol.* **2** (2019), no. 1–2, article no. 1800043.
[142] F. Robicheaux and D. A. Suresh, "Beyond Lowest Order Mean-Field Theory for Light Interacting with Atom Arrays", *Phys. Rev. A* **104** (2021), no. 2, article no. 023702 (12 pages).
[143] D. Plankensteiner, C. Hotter and H. Ritsch, "QuantumCumulants.Jl: A Julia Framework for Generalized Mean-Field Equations in Open Quantum Systems", *Quantum* **6** (2022), article no. 617 (16 pages).
[144] O. Rubies-Bigorda, S. Ostermann and S. F. Yelin, "Characterizing Superradiant Dynamics in Atomic Arrays via a Cumulant Expansion Approach", *Phys. Rev. Res.* **5** (2023), no. 1, article no. 013091 (12 pages).
[145] R. Holzinger, O. Rubies-Bigorda, S. F. Yelin and H. Ritsch, "Symmetry-Based Efficient Simulation of Higher-Order Coherences in Quantum Many-Body Superradiance", *Phys. Rev. Res.* **7** (2025), no. 3, article no. 033203 (10 pages).
[146] C. D. Mink and M. Fleischhauer, "Collective Radiative Interactions in the Discrete Truncated Wigner Approximation", *SciPost Phys.* **15** (2023), no. 6, article no. 233.
[147] H. Hosseinabadi, O. Chelpanova and J. Marino, "User-Friendly Truncated Wigner Approximation for Dissipative Spin Dynamics", *PRX Quantum* **6** (2025), no. 3, article no. 030344 (23 pages).
[148] F. Tebbenjohanns, C. D. Mink, C. Bach, A. Rauschenbeutel and M. Fleischhauer, "Predicting Correlations in Superradiant Emission from a Cascaded Quantum System", *Phys. Rev. A* **110** (2024), no. 4, article no. 043713 (12 pages).
[149] C. Bach, F. Tebbenjohanns, C. Liedl, P. Schneeweiss and A. Rauschenbeutel, "Emergence of Second-Order Coherence in Superfluorescence", preprint, 2024. Online at https://arxiv.org/abs/2407.12549.
[150] A. Asenjo-Garcia, M. Moreno-Cardoner, A. Albrecht, H. J. Kimble and D. E. Chang, "Exponential Improvement in Photon Storage Fidelities Using Subradiance and Selective Radiance" in Atomic Arrays", *Phys. Rev. X* **7** (2017), no. 3, article no. 031024 (36 pages).
[151] N. Skribanowitz, I. P. Herman, J. C. MacGillivray and M. S. Feld, "Observation of Dicke Superradiance in Optically Pumped HF Gas", *Phys. Rev. Lett.* **30** (1973), no. 8, pp. 309–312.
[152] M. Gross, C. Fabre, P. Pillet and S. Haroche, "Observation of Near-Infrared Dicke Superradiance on Cascading Transitions in Atomic Sodium", *Phys. Rev. Lett.* **36** (1976), no. 17, pp. 1035–1038.
[153] H. M. Gibbs, Q. H. F. Vrehen and H. M. J. Hikspoors, "Single-Pulse Superfluorescence in Cesium", *Phys. Rev. Lett.* **39** (1977), no. 9, pp. 547–550.
[154] G. Ferioli, A. Glicenstein, F. Robicheaux, R. T. Sutherland, A. Browaeys and I. Ferrier-Barbut, "Laser-Driven Superradiant Ensembles of Two-Level Atoms near Dicke Regime", *Phys. Rev. Lett.* **127** (2021), no. 24, article no. 243602 (6 pages).
[155] C. Liedl, F. Tebbenjohanns, C. Bach, S. Pucher, A. Rauschenbeutel and P. Schneeweiss, "Observation of Superradiant Bursts in a Cascaded Quantum System", *Phys. Rev. X* **14** (2024), no. 1, article no. 011020 (15 pages).
[156] A. I. Lvovsky, P. Grangier, A. Ourjoumtsev, V. Parigi, M. Sasaki and R. Tualle-Brouri, "Production and Applications of Non-Gaussian Quantum States of Light", preprint, 2020. Online at https://arxiv.org/abs/2006.16985.
[157] M. Walschaers, "Non-Gaussian Quantum States and Where to Find Them", *PRX Quantum* **2** (2021), no. 3, article no. 030204 (68 pages).
[158] L. Lachman and R. Filip, "Quantum Non-Gaussianity of Light and Atoms", *Prog. Quantum Electron.* **83** (2022), article no. 100395 (39 pages).

[159] B. Olmos, G. Buonaiuto, P. Schneeweiss and I. Lesanovsky, "Interaction Signatures and Non-Gaussian Photon States from a Strongly Driven Atomic Ensemble Coupled to a Nanophotonic Waveguide", *Phys. Rev. A* **102** (2020), no. 4, article no. 043711 (7 pages).

[160] R. Loudon, *The Quantum Theory of Light*, Oxford University Press, 2000.

[161] D. A. Steck, "Quantum and Atom Optics". Online at https://atomoptics.uoregon.edu/~dsteck/teaching/quantum-optics/quantum-optics-notes.pdf. Revision 0.16.6 (October 17, 2025).

[162] G. Ferioli, I. Ferrier-Barbut and A. Browaeys, "Emergence of Second-Order Coherence in the Superradiant Emission from a Free-Space Atomic Ensemble", *Phys. Rev. Lett.* **134** (2025), no. 15, article no. 153602 (6 pages).

[163] D. Leibfried, E. Knill, S. Seidelin, et al., "Creation of a six-atom 'Schrödinger cat' state", *Nature* **438** (2005), no. 7068, pp. 639–642.

[164] A. Browaeys and T. Lahaye, "Many-body physics with individually controlled Rydberg atoms", *Nat. Phys.* **16** (2020), no. 2, pp. 132–142.

[165] X. Mi, A. A. Michailidis, S. Shabani, et al., "Stable Quantum-Correlated Many-Body States through Engineered Dissipation", *Science* **383** (2024), no. 6689, pp. 1332–1337.

[166] L. Scarpelli, C. Elouard, M. Johnsson, et al., "Probing Many-Body Correlations Using Quantum-Cascade Correlation Spectroscopy", *Nat. Phys.* **20** (2024), no. 2, pp. 214–218.

[167] A. Bergschneider, V. M. Klinkhamer, J. H. Becher, R. Klemt, L. Palm, G. Zürn, S. Jochim and P. M. Preiss, "Experimental characterization of two-particle entanglement through position and momentum correlations", *Nat. Phys.* **15** (2019), no. 7, pp. 640–644.

[168] V. Gondret, C. Lamirault, R. Dias, C. Leprince, C. I. Westbrook, D. Clément and D. Boiron, "Quantifying Two-Mode Entanglement of Bosonic Gaussian States from Their Full Counting Statistics", *Phys. Rev. Lett.* **135** (2025), no. 10, article no. 100201 (9 pages).

[169] I. Klich and L. Levitov, "Quantum Noise as an Entanglement Meter", *Phys. Rev. Lett.* **102** (2009), article no. 100502 (4 pages).

[170] H. F. Song, C. Flindt, S. Rachel, I. Klich and K. Le Hur, "Entanglement entropy from charge statistics: Exact relations for noninteracting many-body systems", *Phys. Rev. B* **83** (2011), article no. 161408 (4 pages).

[171] H. F. Song, S. Rachel, C. Flindt, I. Klich, N. Laflorencie and K. Le Hur, "Bipartite fluctuations as a probe of many-body entanglement", *Phys. Rev. B* **85** (2012), article no. 035409 (27 pages).